NASA CONTRACTOR REPORT

VAPORIZATION AND DECOMPOSITION KINETICS OF CANDIDATE RE-ENTRY BLACKOUT SUPPRESSANTS IN LOW-PRESSURE FLAMES

by Shelby C. Kurzius and Fredrik H. Raab

Prepared by
AEROCHEM RESEARCH LABORATORIES, INC.
Princeton, N. J.
for Langley Research Center

NATIONAL AERONAUTICS AND SPACE ADMINISTRATION • WASHINGTON, D. C. • AUGUST 1969

VAPORIZATION AND DECOMPOSITION KINETICS OF CANDIDATE RE-ENTRY BLACKOUT SUPPRESSANTS IN LOW-PRESSURE FLAMES

By Shelby C. Kurzius and Fredrik H. Raab

Issued by Originator as TP-181

Prepared under Contract No. NAS 1-7169 by
AEROCHEM RESEARCH LABORATORIES, INC.
Princeton, N.J.

for Langley Research Center

NATIONAL AERONAUTICS AND SPACE ADMINISTRATION

For sale by the Clearinghouse for Federal Scientific and Technical Information
Springfield, Virginia 22151 – CFSTI price $3.00

ABSTRACT

This study provides the first experimental measurements of thermal accommodation coefficients between liquids and high-temperature gas. Beams of uniformly sized droplets were sent across 5 and 10 Torr $H_2/CO/O_2$/air flames and their evaporation rates were photographically determined. Droplet sizes were on the order of the mean free path in the flames (i.e., ~ 100 μm). From the observed evaporation rates, the following translational thermal accommodation coefficients were obtained for combustion gases at about 2500 K: water, 0.76 ± 0.14; perfluoro-octane, 0.17 ± 0.04; Freon E-8, 0.22 ± 0.10. Apparently, only translational energy is effectively transferred from the gas to the liquid; the measured accommodation coefficients are in agreement (within the limits of the data) with predictions based on Baule's classical theory, in which the surface of the condensed phase is regarded essentially as a super-dense gas. Additionally, measurements of the decomposition kinetics of sulfur hexafluoride and perfluoro-octane vapors in 10, 20, 40, and 100 Torr $H_2/CO/O_2$/air flames are reported.

Kinetic implications of the results of this study to engineering evaluation of the use of candidate substances as re-entry blackout suppressants are discussed.

FOREWORD AND ACKNOWLEDGMENTS

This is the final report on NASA Contract NAS1-7169, entitled "The High-Temperature Vaporization and Oxidation Kinetics of Re-Entry Blackout Suppressants." The work herein was sponsored by the Langley Research Center.

It is a pleasure to acknowledge our appreciation to Dr. N.R. Lindblad of the Xerox Corporation for assistance in implementing the acoustically vibrated capillary apparatus, and to 3M Company and E.I. du Pont de Nemours for furnishing property data and samples of perfluoro-octane and Freon E-8, respectively. In addition, we wish to thank R.L. Revolinski for meritorious performance of the decomposition rate experiments, Dr. D.E. Rosner for valuable insights and suggestions, and Dr. W.J. Miller for useful discussion.

CONTENTS

CONTENTS

LIST OF TABLES

LIST OF FIGURES

VAPORIZATION AND DECOMPOSITION KINETICS OF CANDIDATE RE-ENTRY BLACKOUT SUPPRESSANTS IN LOW-PRESSURE FLAMES

By Shelby C. Kurzius and Fredrik H. Raab

AeroChem Research Laboratories, Inc.
a subsidiary of Ritter Pfaudler Corporation
Princeton, N. J.

SUMMARY

The first experimental measurements of thermal accommodation coefficients between liquids and high-temperature gas have been made to facilitate calculations of droplet vaporization rates in low-pressure re-entry flow fields during the communications blackout interval. Beams of uniformly sized droplets were sent across 5 and 10 Torr $H_2/CO/O_2$/air flames and their evaporation rates were photographically determined. Droplet sizes were on the order of the mean free path in the flames (i.e., ~ 100 μm). From the observed evaporation rates, the following translational thermal accommodation coefficients were obtained for combustion gases at about 2500 K: water, 0.76 ± 0.14; perfluoro-octane, 0.17 ± 0.04; Freon E-8, 0.22 ± 0.10. Apparently, only translational energy is effectively transferred from the gas to the liquid; the measured accommodation coefficients are in agreement (within the limits of the data) with predictions based on Baule's classical theory, in which the surface of the condensed phase is regarded essentially as a super-dense gas. Extension of Baule's theory to free molecular supersonic flows (i.e., to directed as opposed to random incident gas molecular fluxes) leads to the following predictions (for spherical droplets) of mean translational thermal accommodation coefficients in high-velocity dissociated air (i.e., N_2/O) plasmas at 5000 K: water, 0.79; perfluoro-octane, 0.30; Freon E-8, 0.47.

Upon vaporization, the electron scavenging efficiency of candidate compounds will depend, inter alia, on their oxidative decomposition kinetics in the prevailing thermal environment. Accordingly, measurements of the decomposition kinetics of sulfur hexafluoride and perfluoro-octane vapors

in 10, 20, 40, and 100 Torr $H_2/CO/O_2$/air flames were undertaken. Flame gases were sampled through quartz probes and analyzed mass spectrometrically. From the resulting decay profiles it is evident that in the low-pressure, high-temperature environments of these studies, sulfur hexafluoride decays suprisingly slowly, whereas perfluoro-octane vapor decays relatively rapidly. The observed decomposition kinetics are expressed in terms of the following rate-determining reactions and rate constants:

$$M + SF_6 \rightarrow \text{Products};$$

$$k = 3 \times 10^{-10} \exp(-70\,000/RT) \text{ cc sec}^{-1} \quad (T > 2500 \text{ K}; \quad p < 40 \text{ Torr})$$

$$H + C_8F_{18} \rightarrow \text{Products};$$

$$k = 4 \times 10^{-11} \exp(-4000/RT) \text{ cc sec}^{-1}$$

Interim SF_6 and C_8F_{18} vapor decomposition mechanisms and rate constants for use in low-pressure re-entry flow field blackout calculations are suggested.

INTRODUCTION

A major purpose of current NASA Langley re-entry communications research is to understand in depth (and thereby enable optimization of) the mechanisms by which externally injected atomized liquid jets and their vapors interact with the plasma sheath surrounding high-altitude re-entry vehicles to alleviate rf communications interference.[1-4*] To help attain this goal, AeroChem undertook the present study to generate required information on (1) the thermal accommodation coefficients of liquids of interest in re-entry communications blackout suppression and (2) the kinetics of oxidative decomposition of electrophilic vapors of candidate liquids in low-pressure, high-temperature environments. Such information was previously unavailable and is essential in (1) the calculation of droplet evaporation rates in free and near free molecule regimes and (2) the evaluation of droplets as distributed sources

* Superscripts indicate reference numbers (see page 33).

of (perhaps) chemically short-lived, strongly electron-attaching molecules in re-entry flow fields typified by those encountered[1-4] by Project RAM vehicles during the communications blackout interval. Such evaluation is the subject of additional studies, now in progress, to which the present results are intended to provide useful inputs.

SYMBOLS

a	intermolecular spacing, cm
A	Arrhenius rate constant [k = A exp (- E/RT)] pre-exponential factor, cc molecule^{-1} sec^{-1}
Ä	angstrom (10^{-8} cm)
b	liquid structural parameter defined by $b = a/\sigma_M$
B	dimensionless mass flux defined by Eq. (8)
c_p	gas specific heat, cal g^{-1} K^{-1}
d	droplet diameter, cm
e	elementary charge, C
E	Arrhenius rate constant [k = A exp (- E/RT)] activation energy, cal mole^{-1}
h	Planck's constant, erg sec
$\Delta H^o_{f,0}$	standard heat of formation at 0 K, cal mole^{-1}
k	Boltzmann constant, erg K^{-1} molecule^{-1}; or rate constant, cc molecule^{-1} sec^{-1}
ℓ	gas mean free path, cm
L	latent heat of vaporization, cal g^{-1}
m	gas molecular mass, g
$\overline{m}$	kinetic mean gas molecular mass defined by Eq. (2), g
$\dot{m}''$	net mass flux, g cm^{-2} sec^{-1}
M	liquid molecular mass, g; or non-specific gas species
n	gas number density, molecules cc^{-1}
n_s	gas number density (at T_s) at liquid surface saturation vapor pressure, molecules cc^{-1}

N_A	Avogadro's number, molecules $mole^{-1}$
Nu	Nusselt number
Nu_0	Nusselt number at zero net mass flux
p	pressure, Torr
Pr	Prandtl number
$\dot{q}''$	net heat flux, cal cm^{-2} sec^{-1}
R	universal gas constant, cal K^{-1} $mole^{-1}$
Re	Reynolds number
t	time, sec
T	temperature, K
v	mean thermal velocity, cm sec^{-1}
$\bar{v}$	kinetic mean thermal velocity defined by Eq. (2), cm sec^{-1}
x	mole fraction
α_L	Langmuir evaporation coefficient defined by Eq. (11)
α_T	translational thermal accommodation coefficient
$\alpha_{T,D}$	translational thermal accommodation coefficient for directed incident gas flux
δ	boundary layer thickness, cm
ϵ	Lennard-Jones molecular potential interaction energy parameter, erg $molecule^{-1}$
λ	gas thermal conductivity, cal K^{-1} cm^{-1} sec^{-1}
ν	reflection coefficient of gas molecules striking liquid surface
ρ	density, g cc^{-1}
σ	Lennard-Jones molecular potential collision diameter, cm
Σ	summation
ϕ	flame equivalence ratio: ratio of stoichiometric to actual oxidizer/fuel ratios
Ω_μ	reduced collision integral for viscosity (see Ref. 29, p. 524)

Subscripts

D	pertaining to directed (as opposed to random) incident gas fluxes
E-8	Freon E-8
HS	hard sphere
i	gas species i (arbitrary)
L	pertaining to bulk liquid
m	pertaining to incident gas molecule
M	pertaining to liquid molecule
s	pertaining to surface
T	thermal
1	pertaining to fictional gas envelope one mean free path from liquid surface
3	volume mean
∞	free stream

Superscript

(1)	pertaining to single gas molecule-liquid molecule encounters

Miscellaneous

$\pm$	quantities following $\pm$ are standard deviations
[i]	number density of species i, molecules cc^{-1}
$\overline{\quad}$	mean quantity

I. BACKGROUND

For conceptual purposes, representative high-altitude re-entry shock layer parameters of present interest can be considered to be approximately as follows:[5]

p : 10 Torr

T : 5000 K

ℓ : 100 μm

d_3 : 10 μm

As discussed in Ref. 5, predicted atomized jet mean droplet sizes in representative flow fields of interest are significantly smaller than prevailing mean free paths. With respect to gas-droplet interactions, the flows of present interest are thus essentially free molecular. In such flows, droplet evaporation rates are directly proportional to the thermal accommodation coefficient α_T of the incident high-velocity, high-temperature gases on the relatively cool liquid surface.[6,7] However, a survey of the literature covering the period from the conception of the thermal accommodation coefficient by Knudsen[8] in 1911 to the present discloses only <u>one</u> quantitative measurement of α_T for liquid surfaces: Alty and Mackay[9] found that α_T for water vapor molecules at 10°C incident on a water surface at 0°C is 1.0. As can be inferred, for example, from the comprehensive reviews of thermal accommodation coefficients of gases with <u>solid</u> surfaces by Wachman et al.,[10,11] Alty and Mackay's result can not be extrapolated to high gas temperatures with confidence since α_T is in general a complex function of temperature. Consequently, in high-altitude re-entry flow fields (in which the temperature difference between the incident gas and evaporating liquid surface is several thousand degrees) a serious lack of detailed knowledge regarding actual free molecule flow evaporation rates has existed.

Similarly, measurements at <u>low</u> pressures of high-temperature oxidative decomposition kinetics of electrophilic vapors of potential liquid re-entry blackout suppressants have not previously been made. The kinetics of SF_6 decomposition had, however, been studied in flames by Fenimore and Jones[12] at pressures from 80 to 160 Torr and temperatures from 1300 to 1940 K. Since the present study was begun, SF_6 decomposition in shock-heated argon has been investigated by Modica[13,49] (at 1060 Torr, between 1700 and 2100 K) and by Bott, Thompson, and Jacobs[14] (between 100 and 3400 Torr and 1700 and 2050 K). The latter results and their relation to those obtained in the present study at lower pressures and higher temperatures are discussed in Section III. B.

II. EXPERIMENTAL APPROACH

A. Droplet Evaporation Measurements

In order to measure evaporation rates of freely moving small droplets, it is necessary to either (1) follow the course of a single droplet in flight by high-speed cinematography or stroboscopic still photography or (2) using a beam of uniformly sized droplets of known velocity, perform single-exposure measurements at spatially separated stations. The former methods require (in practice) that a droplet flight distance sufficiently long for appreciable evaporation to occur be compatible with the film format at a magnification high enough to permit accurate size measurement of the images. Since this requirement was impossible to fulfill in the present studies, we employed the latter method.

Various techniques[15-19] for the production of uniformly sized liquid droplets have been developed since 1950, most recently by Schneider et al. These techniques are based on the well-known results of Lord Rayleigh[20] concerning the dynamic instability of a cylindrical liquid jet to which a sinusoidal wave disturbance is imparted (by mechanical vibration of the capillary). We have followed the method of Schneider et al.,[18, 19] which involves the use of an audio generator and power amplifier to drive a piezoelectric transducer at approximately the Rayleigh instability frequency of the jet. A glass capillary carrying the liquid is secured transverse to a simple beam-mounted piezoelectric crystal (see Fig. 1). When the crystal is vibrated, the liquid jet rapidly disintegrates into a beam of (initially) extremely uniformly sized and spaced droplets, whose number per second is equal to the driving frequency (see Fig. 2). Droplet size can be varied within certain narrow limits at constant mass flow rate by varying the oscillator frequency, or capillaries of different diameters can be used to obtain various droplet sizes. With such a uniform beam, it is clearly unnecessary to measure the evaporation rate of one particular droplet since, barring coalescence due to aerodynamic drag or turbulent wake effects, each droplet will have an identical history along a given trajectory in a given environment. (It will be seen below, however, that coalescence did occur to varying degrees in some cases.)

A schematic view of our apparatus (much of which has been described previously[21]) is given in Fig. 3; injection parameters and flame characteristics are given in Tables I and II, respectively. The capillaries were drawn

from 3 mm glass tubing, scored with a diamond stone and broken off, leaving flat, smooth, sharp-edged orifices which were accurately measured by photomicrography. The piezoelectric transducers were Clevite PZT-5B Bimorphs, 0.61 mm thick and silver-plated. In-line filtration of the liquids was by a Millipore 5 μm Teflon filter. Beams of droplets (distilled water, perfluorooctane,* and Freon E-8;† see Table III for liquid properties) were initiated ~ 4 cm from the burner's edge and were directed through the centers of 19 cm-diam flat pre-mixed flames, 10 cm downstream of the (uncooled) burner top. To avoid flashing of the C_8F_{18} at the orifice, it was necessary to cool the capillary; this was done by wrapping it in water-soaked cotton. Upon evacuation of the chamber the water froze, providing satisfactory cooling for the duration of a typical run. Freon E-8, on the other hand, has such a high viscosity that it was necessary to heat the capillary in order to get this liquid out at all; this was accomplished with a coil of resistance-heated nichrome wire.

The flames used were H_2/O_2, H_2/air, CO/O_2, and CO/air, all of which had an equivalence ratio ϕ of 7/8 (it was necessary, however, to add 1.3 vol. % CH_4 to the CO flames to stabilize them, since hydrogen atoms are essential to CO combustion[22]). Chamber pressures were either 5 or 10 Torr, yielding Knudsen numbers in the range 0.3 to 1.5 for the droplet sizes used, based on water molecule mean free paths in the various flames. (Preliminary experiments performed at 2 and 20 Torr did not yield useful data.) An optical system for single-exposure, bright-field, ultrahigh-speed flash photography at a magnification of ~ 4.0 was mounted perpendicular to the jet axis and could be traversed in any direction. As in our previous study,[5] the light source was an EG &G Model 549 Microflash, but the optics used in the present work consisted of a Miranda G 35 mm SLR camera body with a Schneider 300 mm f/5.6 Comparon enlarging lens having optimum resolution at a magnification of 4. We used Kodak High Contrast Copy film, developed in Acufine and printed on Kodak Polycontrast F paper. Details of the calibration of this technique for the measurement of microscopic droplet sizes are given in Ref. 5.

A significant deviation in our work from the method of Schneider et al.[18,19] is that we did not use their very sophisticated electrostatic charging technique for pulsing single droplets or small groups of droplets out of the main beam. To do so would have required a prohibitively large investment in time and funds to achieve the high accuracy of droplet trajectory

---

* 3M Company, St. Paul, Minn.

† E.I. du Pont de Nemours, Wilmington, Del.

over a relatively great distance (~ 18 cm) required in our experiments. This is especially true in consideration of the fact that the capillary assembly was inside a vacuum chamber in a hot, extremely corrosive environment (during the C_8F_{18} and Freon E-8 runs, virtually everything in the chamber was attacked to varying degrees by hydrogen fluoride generated in the flames). Because of the desirability of pulsing single droplets into the flames to avoid possible coalescence effects and flame perturbation, we put considerable effort into the mechanical chopping of the droplet beam by means of a high-speed slotted disc placed between the capillary and the burner. Although it was possible, with the correct combination of disc thickness, slot width, and angular velocity, to isolate single droplets at ~ 1 msec intervals, these droplets followed such erratic trajectories -- apparently due to the severe aerodynamic turbulence generated by the disc (even at 5 Torr) -- that they were impossible to locate (photographically) in the flames. Hence, this approach was ultimately abandoned.

Even without the chopper, beam trajectory remained a most serious problem. The jets in our experiments frequently tended to "walk" in the vacuum chamber (i.e., to deviate from their intended trajectories in a random manner and for no apparent reason) enough to carry them up to a centimeter off center in any direction at the midpoint of the flame. Horizontal deviation was the most troublesome, since it almost invariably put the droplets out of focus; the droplets were too small to be seen through the camera viewfinder even when in focus. (Acceptable focal depth-of-field[5] is a function of droplet diameter; in these experiments it ranged from 3 mm for the smallest to 9 mm for the largest droplets.) In addition to the effects of inherent jet instability, the droplets tended to be blown vertically upward by the flame gases, along sweeping curves which varied with the flames; this motion required compensatory tracking with the optics and burner. These combined factors necessitated a brute-force experimental procedure, wherein the effective photographic area (~ 6 x 9 mm) was swept up and down and the focus swept in and out at a given lateral position in the flame in order to find the droplets and get them into acceptable focus. The net result was a frustratingly low efficiency in data collection, typically 1 to 2% (i.e., approximately 50 to 100 photographs were required for each one which proved useful).

Two lateral photographic stations located 4 cm on either side of the center of the flame were employed for each liquid in each flame. The droplet trajectory between measuring stations was thus symmetrical with respect to the radial temperature profile in the flame and comprised the central 8 cm

of a 19 cm-diam flame. (On the basis of thermocouple radial temperature traverses, we estimate that the mean gas temperature in this region is ~ 90% of the centerline temperature.)

Figures 4 through 6 are illustrative of the results obtained under typical conditions. Prevailing local droplet velocities were calculated from their known production frequencies and the observed droplet spacings on the "beam" photographs. Velocities so measured agreed satisfactorily with those predicted from the measured volumetric flow rates and vena contracta diameters;[16] they decayed by approximately 4 to 8% between stations.

A few points concerning Figs. 4 through 6 are worth mentioning. In all cases, droplet motion is from right to left. Station No. 1 in the photographic plane is 4 cm to the right of center of the burner axis (i.e., the droplets are entering the measuring zone); Station No. 2 is 4 cm to the left of center. In most cases, the beam was dispersed into a 2-dimensional vertical spray (with only slight lateral dispersion) by the time it reached the left-hand side; this is clearly evident in Figs. 4B and 5B. Note, however, that in Fig. 5A (Freon E-8 at Station No. 1), the beam is already quite ragged, a phenomenon which occurred fairly consistently with this highly viscous liquid and was presumably due to some unusual jet instability at the capillary tip. The C_8F_{18} photographs are of particular interest: note that in Fig. 6A there is no flame, demonstrating that in the absence of this perturbation, the beam maintains its integrity over a great distance (~18 cm -- ~ 2500 orifice diameters -- from the capillary tip). Figure 6B illustrates the problem of droplet coalescence, which was quite severe with C_8F_{18}; note that two droplets are visible which are noticeably smaller than the others--these are un-coalesced droplets, as deduced from the analysis of many such photographs. The degree to which coalescence has occurred can be estimated by counting the number of droplets per frame; since there is no operative mechanism other than evaporation by which droplets from the original beam can become smaller, the measurement (from numerous photographs) of these minimum-sized droplets is justified.

As a final note, Fig. 7 illustrates a particularly vexing problem encountered with these jets, namely satellite jet formation.[19] Unless the voltage on the transducer is carefully tuned, these satellites appear (often several at a time) and spray off the capillary tip in random directions. (The photograph shown is a rare instance of virtual coaxiality of the main and satellite jets.) Even when the voltage is held quite constant, the operating

characteristics of the capillary assembly tend to drift slightly, causing the satellites to appear and disappear unpredictably. A detailed experimental and theoretical treatment of the production of beams of uniformly sized droplets is given in Ref. 19.

B. Decomposition Kinetics Measurements

The experimental approach followed in this phase of the present study was the standard one for the sampling of neutral species from flames, as described in the treatise by Fristrom and Westenberg.[22] This technique involves the insertion of a quartz sampling probe into the flame gases and continuously withdrawing a sample which is channeled directly to the inlet of a mass spectrometer or some other suitable analytical instrument. Chemical species concentration profiles can be obtained by varying the burner-to-probe distance,which corresponds to changing time along the flame reaction coordinate.*

A schematic of our apparatus is shown in Fig. 8. Flat, pre-mixed, 9.1 cm-diam flames (see Table IV) were burned at pressures from 10 to 100 Torr. Sampling was performed at the centers of the flames over distances up to 5 cm from the burner top. Sulfur hexafluoride† was metered by a gas microburet and pre-mixed with the flame gases; perfluoro-octane liquid was metered by a syringe pump, vaporized in a heated venturi injector, and likewise pre-mixed. Attempts to introduce Freon E-8 vapor into the flames were unsuccessful due to the extremely low vapor pressure of this liquid (see Table III). It should be noted that instead of the conventional fine-drawn quartz capillary probe tip used in most flame studies, we found it necessary to use a blunted tip‡ with a small orifice (~ 50-150 μm diam) at its center; this was done to cool the tip and thereby slow the otherwise

---

* This technique was also employed by Fenimore and Jones[12] in their study of SF_6 decomposition kinetics.

†The Matheson Company, East Rutherford N.J.; purity was greater than 98.0 vol. %.

‡Satin-surface Vitreosil, Thermal American Fused Quartz Co., Montville, N.J.

rapid attack of hydrogen fluoride on the probe. Cylinders of copper foil inserted into the probes to catalyze radical recombination reactions were employed (pressures inside the probe were ~ 20 times lower than outside--i.e., ~ 0.5-5 Torr). In experiments performed with and without these inserts, they were found to have little effect on apparent SF_6 decomposition rates.

The mass spectrometer employed was an AeroVac Model 685, equipped with a Model 514-01 high-temperature electromagnet system. This instrument is of the magnetic deflection type, with a mass range of 1-500 amu, a resolution of 250 amu,and a sensitivity nominally in the 10^{-13} Torr range. It employs 72 eV ionizing electrons; ion acceleration is variable between 20 and 750 V, with a hyperbolic mass separation distribution. In the present study, useful peak intensities were not obtained in sampled flame gases beyond 150 amu; mass calibration was done with H_2, N_2, Ar, and SF_6.

The cracking pattern of perfluoro-octane has not previously been reported. It consists (for 72 eV electrons) of seven relatively strong ion peaks, listed below in decreasing order of arbitrary intensity units:

Species	Mass, amu	Intensity
CF_3^+	69	100
$C_2F_5^+$	119	17
$C_3F_5^+$	131	15
$C_2F_4^+$	100	13
CF^+	31	11
$C_3F_8^+$	188	2.5
$C_5F_{11}^+$	269	1.8

In addition to these, there are dozens of minor peaks* which are of no use in kinetic studies; the parent peak, at mass 438, was extremely weak. Time and funds did not permit evaluation of the effects of modifying the instrument to reduce the energy of the ionizing electrons from 72 eV. For our purposes, the two predominant masses, 69 and 119, were the most suitable for tracking in the flames.

III. RESULTS AND DISCUSSION OF PRESENT INVESTIGATION

The results of these unique studies are, we believe, both significant in their implications and -- in some respects -- surprising (e.g., the unexpectedly slow observed rates of SF_6 decomposition; Section III.B.1). It is appropriate to point out at the onset of this discussion, however, that in a very real sense the present investigation must be regarded as prefatory to more extended and refined studies. Thus, measurements of free molecular droplet evaporation rates in less complex environments than the present flames and less subject to intrinsic depth-of-field/jet-instability accuracy limitations[5] (as, e.g., by the use of holography[23]) should be actively pursued in future studies. Although AeroChem is presently exploiting techniques discussed by Gaydon[24] to spectroscopically measure low-pressure flame rotational temperatures, the techniques were not available for this study and we were obliged to use calculated adiabatic flame temperatures and compositions in the interpretation of our results.

Thermocouple centerline temperature traverses employing junctions of different diameters were taken in several of the flames studied. However, after analysis the data were rejected for the following reasons: (1) catalytic heating due to atom and radical recombination could <u>not</u> be satisfactorily suppressed (silica coatings[25] did not help, as these were (somewhat erratically) vaporized in the high-temperature flames of the present study) and (2) theoretical interpretation of the data indicates strongly that the still

---

* Note that the liquid consisted of only 63 vol.% n-C_8F_{18}; of the residue, 27% consisted of branched-chain isomers. The remaining 10% comprised homologous perfluoroalkanes.

further complicating effects of free molecule limitations on incident thermal fluxes to even relatively large (i.e., 1020 μm diam) radiation-cooled thermocouple probes are severe in these flames. (Characteristic Knudsen numbers were on the order of 0.1.) After considerable experimental and analytical effort, we were reluctantly forced to the conclusion that the use of thermocouples is inadequate to unambiguously determine true flame temperatures at low pressures. Indeed, use of previously recommended[25] (continuum) concepts to infer true peak flame temperatures in a $7CO/4O_2$ flame at 10 Torr from thermocouple measurements (with wires of 255, 510, and 1020 μm diam) leads to values ranging from 2100 to 2700 K, depending primarily on wire size. (These are to be compared with a calculated adiabatic equilibrium flame temperature of 2541 K.) Simple extrapolation to zero junction size is not reliable, primarily because free molecule limitations become most severe for the smallest sizes.

A. Thermal Accommodation Coefficients

Selected nominal properties of the liquids employed in these studies are shown in Table III; characteristics of the flames (at 10 Torr) are shown in Table II. The property evaluations given are based largely on (1) JANAF thermochemical data,[26] (2) Svehla's[27] and Moelwyn-Hughes'[28] compilations, (3) combinatorial and estimating techniques described by Hirschfelder, Curtiss, and Bird[29] and Reid and Sherwood,[30] and (4) manufacturers' literature for the fluorocarbon liquids.[31,32] In particular, the Lennard-Jones collision diameters of perfluoro-octane and Freon E-8 have been estimated from the parachor (Ref. 29, p. 356); the intermolecular spacing in the bulk liquids has been calculated on the basis of Clusius and Weigand's model.[33]

Droplet evaporation rates observed in the present experiments (using the techniques discussed in Section II.A) are summarized in Table V; their interpretation in terms of free molecule incident heat flux-limited evaporation kinetics is summarized in Table VI. The following quasi-steady-state theory has been utilized in the interpretation of the observed droplet evaporation rates:

1. Droplet evaporation rate theory. - Figure 9 shows the conceptual heat transfer model of an evaporating droplet used here in theory formulation. Neglecting radiation and chemical reaction, we regard the heat transfer flux

to the droplet surface $\dot{q}_s''$ to be determined* by the free molecular thermal flux originating (conceptually) from a spherical gas envelope at temperature T_1, located one mean free path ℓ_1 from the droplet surface. Adopting Brock's[34] postulate (justified a posteriori by the present experiments) that internal degrees of freedom remain essentially unequilibrated in the very short contact time between incident inert molecules and the droplet surface, translational energy transfer is the dominant heat transfer process, with the result that

$$\dot{q}_s'' = \bar{\alpha}_T n_1 (\bar{v}_1/4) 2k(T_1 - T_s) \tag{1}$$

In Eq. (1), 2k is the mean translational specific heat of molecules emerging from the gas;[7] the term $(T_1 - T_s)$ is seen to be the "temperature jump;"[35] the term $\bar{v}$ is an effective kinetic mean thermal velocity, defined here by

$$\bar{v} = \sum_i x_i v_i = \left(\frac{8kT}{\pi \bar{m}}\right)^{1/2} \tag{2}$$

which also defines $\bar{m}$, an effective kinetic mean molecular mass.

Under quasi-steady-state conditions, the flux given by Eq. (1) is balanced by the evaporation heat flux, i.e.,

$$\dot{q}_s'' = (\rho_s L_s/2) \left[\frac{-d(d)}{dt}\right] \tag{3}$$

Combination of Eqs. (1) and (3) yields the following results, through the use of which $\bar{\alpha}_T$ was calculated† from the observed evaporation rates:

---

* At low incident speed ratios (drift to mean thermal velocity), as in the present experiments.

†Thus, we have implicitly assumed that steady-state droplet temperatures were attained by the time droplets reached Station No. 1, which was immersed ~ 6 cm in the flame, i.e., ~ 10 cm from the capillary (see Fig. 3). Estimates of sensible vs latent heat requirements indicate that at the observed levels of heat flux this assumption is reasonable.

$$\bar{a}_T = \left[\frac{\rho_s L_s}{n_1 \bar{v}_1 k (T_1 - T_s)}\right] \left[\frac{-d(d)}{dt}\right] \tag{4}$$

The temperature T_1 in Eq. (4) has been calculated by reasoning that $\dot{q}''_s$ is maintained by the effective convective thermal flux arriving at the spherical envelope (at T_1; see Fig. 9) from the external gas, i.e.,

$$\dot{q}''_s = \dot{q}''_1 \left(\frac{d + 2\ell_1}{d}\right)^2 \tag{5}$$

where, from simple film theory,[36]

$$\dot{q}''_1 = \left(\frac{Nu\,\lambda}{d + 2\ell_1}\right)(T_\infty - T_1) \tag{6}$$

In Eq. (6), the prevailing transfer coefficient Nu is related[36] to the transfer coefficient in the absence of net mass transfer Nu_0 by

$$Nu/Nu_0 = [\ln (1 + B)]/B \tag{7}$$

where

$$B = [c_p(T_\infty - T_1)]/L_s \tag{8}$$

and, for spheres,

$$Nu_0 = 2 + 0.6\,Re^{1/2}\,Pr^{1/3} \tag{9}$$

Equation (9) is known[37] to be valid (with $\ell \ll d$) for spheres sharply bounded at a radius of d/2. We assume it valid also for spheres bounded by a kinetic sheath (see Fig. 9)--i.e., a "sink" surface--of radius $(d + 2\ell)/2$; this premise seems reasonable when (as in the present experiments) the forced convection contribution to Nu_0 is relatively small (i.e., when $0.6\,Re^{1/2}\,Pr^{1/3} \ll 2$). After rearranging terms, the following equation relating T_1 to observed evaporation rates is obtained:

$$\ln\left[1 + \frac{c_p(T_\infty - T_1)}{L_s}\right] = \left(\frac{d\,\rho_s\,c_p}{2\,Nu_0\,\lambda}\right)\left(\frac{d}{d + 2\ell_1}\right)\left[\frac{-d(d)}{dt}\right] \tag{10}$$

Equation (10) has been used to calculate the values of T_1 shown in Table VI, with λ and c_p evaluated at the arithmetic mean film temperature (i.e., at $(T_1 + T_\infty)/2$). As is evident, heat transfer to the droplet

surfaces is essentially determined by kinetic limitations in the present experiments. This is indicated most clearly by the high ratios of $(T_l - T_s)/(T_\infty - T_l)$. (In the limit of continuum flux limitation, the latter ratio would approach zero.)

Finally, neglecting reflected (i.e., incident) fluxes of vaporized molecules for present purposes, the evaporative heat flux may also be written in terms of the molecular flux from the droplets:

$$\dot{q}''_s = L_s \dot{m}''_s = \alpha_L n_s (v_s/4) L_s N_A M \qquad (11)$$

where α_L is the Langmuir evaporation coefficient. By combining Eq. (11) and Eq. (1) and rearranging terms, the following equation for the steady-state ratio of p_s (the saturation partial pressure at T_s) to the ambient pressure p_∞ is obtained:

$$\frac{p_s}{p_\infty} = \left(\frac{\bar{\alpha}_T}{\alpha_L}\right)\left(\frac{T_s M}{T_l \bar{m}}\right)^{1/2}\left[\frac{2R(T_l - T_s)}{L_s N_A M}\right] \qquad (12)$$

Equation (12) yields p_s and therefore the droplet surface temperature for a given set of conditions. Calculated values of T_s shown in Table VI were obtained from Eq. (12), using a value of unity for α_L (on the basis of the most recent experimental evidence[38]) and using the theoretical values of $\bar{\alpha}_T$ also shown in Table VI (these values are discussed in Section III.A.5). An interesting result of these calculations is that T_s for water droplets is predicted to be <u>below</u> the equilibrium freezing temperature in the flame environments of the present study; for example, 23 K of supercooling is predicted for water droplets in the CO/O_2 flame at 5 Torr (see Table VI). That superficial crystallization did <u>not</u> occur was evidenced by the observation of droplet coalescence in the flames (Section II.A). This is consistent with observations of Kuhns and Mason[39] which indicate that supercoolings in excess of 30 K are required to freeze water droplets of ~ 100 μm diameter.

2. <u>Water</u>.- As can be seen in Tables V and VI, observed rates of diameter decrease were slowest for water droplets; their measurement was made difficult principally by the smallness of the observed changes. Standard deviations of $-\overline{\Delta d}$, the mean observed diameter change, are included in Table V for water; they are seen to be an appreciable fraction

(from 8 to 32%) of the mean and thus account for the rather appreciable scatter in the results shown in Table VI. No meaningful trend with either composition, temperature, or pressure can be extracted from the experimental values of $\bar{\alpha}_T$ shown in Table VI; the results are summarized by

$$\bar{\alpha}_T = 0.76 \pm 0.14$$

3. Perfluoro-octane.- Significantly faster rates of diameter decrease were observed with this liquid than with water. The measurements summarized in Tables V and VI are expressed by

$$\bar{\alpha}_T = 0.17 \pm 0.04$$

4. Freon E-8.- The low purity (Table III) of this high-boiling liquid mixture (and hence the probability of partial fractionation during the course of the experiments) and the difficulties in stabilizing highly viscous Freon E-8 droplet beams (Section II.A) were additional complicating factors in these experiments. The measurements summarized in Tables V and VI are expressed by

$$\bar{\alpha}_T = 0.22 \pm 0.10$$

5. Discussion.- The present experiments have shown quite clearly that the apparent translational thermal accommodation coefficients of liquids subject to collision fluxes of high-temperature gases can differ significantly from unity, although, equally clearly, a need exists for more refined experiments. Based on the present results (Table VI), in which (1) $\bar{\alpha}_T$ is apparently bounded by unity* and (2) no appreciable trends toward enhancement in measured values of $\bar{\alpha}_T$ are observed in going from air flames, with relatively low atom and free radical concentrations, to oxygen flames, where the concentrations are relatively high (Table II), we infer that chemical and other contributions to incident heat fluxes are relatively minor. Thus, we conclude that only translational energy transfer from the gas to the liquid is required to describe incident thermal fluxes.

---

* In this work, $\bar{\alpha}_T$ has been interpreted as corresponding to translational accommodation only. Thus, if chemical, rotational, vibrational, or electronic contributions were significant, experimental values of $\bar{\alpha}_T$ would not necessarily be bounded by unity.

As yet no theories of thermal accommodation between gases and liquids have been specifically formulated. We will show, however, that the earliest theoretical effort (by Baule[40] in 1914) to describe gas-solid lattice thermal accommodation, although long since discredited, was in fact based on a rather good model for high-temperature gas-liquid thermal accommodation. Indeed, Baule's theory predicts gas-liquid thermal accommodation coefficients in agreement with the present results, within the error limits of the data.

Baule applied classical theory to a model in which gas and surface molecules behave like elastic spheres. In particular, lattice interactions are presumed to be negligibly weak during gas-surface encounters; thus Baule's concept of the surface is essentially that of a super-dense gas. Objections to applying Baule's model to low-temperature gas-solid lattice encounters are severe, as discussed elsewhere.[10] However, for high-temperature gas-liquid encounters:

1. Classical rather than wave mechanical theory should be applicable, since the mean de Broglie wavelengths ($h/m_i v_i$) of the incident gas molecules are small relative to liquid intermolecular spacings. (For example, at 2000 K, the mean de Broglie wavelength of N_2 is 0.116 Å.)

2. For collisions not significantly involving chemisorption phenomena (as, apparently, in the present experiments), essentially elastic initial gas-liquid encounters can be anticipated, provided that incident thermal energies (2RT cal mole^{-1} for kinetic incident fluxes[28]) are large relative to prevailing heats of physical adsorption (on the order of kcal mole^{-1}). Elastic encounters will also result if stabilization of sorption complexes by dissipation of sorption heats to intervening third bodies is not favored during the lifetime of the complexes. Although the limitations of applying the elastic collision assumption to high-temperature gas-liquid encounters are not now known, we infer a posteriori from the essential (statistical) agreement between experiment and theory evident in Table VI that the elastic primary collision model is a reasonably good one.

3. Baule's assumption that each surface mass point behaves as an independent elastic suspension (with respect to its neighbors) during gas encounters has been shown[10] to be unquestionably a poor one for gas-solid lattice interactions. However, when the dense phase is relatively unstructured --as are liquids--Baule's assumption is much more likely to be correct.

Baule first analyzed energy accommodation for single (i.e., primary) encounters of arbitrary temperature distribution function, with the often-quoted result that

$$a_T^{(1)} = \frac{2mM}{(m + M)^2} \tag{13}$$

He then made the intuitive approximation that all incident gas molecules which are not reflected from the surface by their first encounter with a surface layer molecule become enmeshed in the dense phase and leave it only after becoming effectively completely accommodated to the surface temperature. Thus, if $\nu^{(1)}$ is the reflection coefficient for incident molecules experiencing only one encounter with a surface molecule,

$$a_T = a_T^{(1)} + \left(1 - a_T^{(1)}\right)\left(1 - \nu^{(1)}\right) \tag{14}$$

In an elegant derivation, the results of which appear to have been generally overlooked, Baule next evaluated $\nu^{(1)}$. If we (1) approximate the effective gas-liquid molecular potential function by a Lennard-Jones potential, (2) substitute modern gas kinetic parameters for the effective hard-sphere collision diameter appearing in Baule's theory, i.e., make the substitution

$$(\sigma_m + \sigma_M)^2_{HS} = (\sigma_m + \sigma_M)^2 \Omega_\mu \tag{15}$$

where Ω_μ is the appropriate collision integral (evaluated at the incident gas temperature) compiled by Hirschfelder et al.,[29] and (3) regard the intermolecular dense phase surface spacing a_s not as an adjustable parameter (as did Baule) but as the average bulk dense phase intermolecular spacing a_L,

$$a_s \equiv a_L = b_L \sigma_M \tag{16}$$

then Baule's result for $\nu^{(1)}$, evaluated for thermal incident fluxes obeying a cosine distribution law, may be rewritten as

$$\nu_T^{(1)} = \frac{\pi\Omega_\mu}{8\, b_L^2}\left(1 + \frac{\sigma_m}{\sigma_M}\right)^2 \left\{ \frac{M - m}{2M} + \ln\left[\frac{4b_L}{\left(1 + \frac{\sigma_m}{\sigma_M}\right)\sqrt{\Omega_\mu}} \right] \right\} \tag{17}$$

Values of $\alpha_T^{(1)}$, $\nu_T^{(1)}$, and α_T predicted by the above theory for various incident gas molecules at 2500 K and for the liquids studied in the present investigation are compiled in Table VII. Finally, values of $\bar{\alpha}_T$ computed from

$$\bar{\alpha}_T \bar{v} = \sum_i x_i v_i \alpha_{T,i} \qquad (18)$$

are shown in Table VI for the experimental environments of the present study. Although refinements to both the present measurements and to Baule's theory (as here reinterpreted) can and undoubtedly will be made in future work, the present results do appear to be compatible with theoretical predictions based on Baule's classical framework.

B. Decomposition Kinetics

Characteristics of the flames employed in the SF_6 and C_8F_{18} decomposition kinetics studies are shown in Table IV. We note that the flames used in both studies were identical except for added SF_6 or C_8F_{18}; equilibrium calculations (Table IV) were, however, made only for the flames containing SF_6. We also note that argon (0.2 to 1.4 vol.%) was usually added to these flames for mass identification purposes; in runs performed both with and without argon, there were no significant changes in the observed kinetics.

1. Perfluoro-octane.- Vapors of this substance decomposed rapidly in the environments of the present study. Representative decay profiles (in an H_2/O_2 flame at 10 Torr) are shown in Fig. 10. As previously mentioned (Section II. B), C_8F_{18} was necessarily monitored indirectly in the flames via the dominant CF_3^+ and $C_2F_5^+$ peaks from its cracking pattern. Relative contributions of parent (C_8F_{18}) and daughter fragments to these peaks cannot be separated; we note, however, that each peak decays at essentially the same rapid rate (see Fig. 10) with little change in the $CF_3^+/C_2F_5^+$ peak ratios as the decomposition proceeds. We infer from these observations that daughter free radical fragments which could contribute CF_3^+ and/or $C_2F_5^+$ to the ion spectrum are short-lived in the flames

studied.* According to this interpretation, CF_3^+ in the spectrum is likely to be a reasonable indicator of the C_8F_{18} concentration in the environments of present interest,although this point requires further verification. It is important to note, however, that significant quantities of CF_2O were produced in the CO flames (see Fig. 11, which shows representative results obtained in a CO/O_2 flame at 40 Torr), although the kinetics of CF_2O reactions were not quantitatively studied. CF_2O was not detected in the H_2/O_2 flame (Fig. 10).

Observed decomposition rates inferred from the essentially linear diffusion-corrected semi-log slopes of the decay profiles and the flame velocities (following the procedures discussed in Ref. 21) are summarized in Table VIII. Estimates of H atom concentrations in the flames with additive were obtained as follows:

1. In the H_2/O_2 flame, [H] was inferred from the ratio of the residual (i.e., final)H_2 in the probe-sampled gases (see Fig. 10) to the initial H_2 mole fraction; since H sampled from the flame recombines in the probe, a correction was applied on the basis that H and H_2 in the residual hydrogen are in their equilibrium ratio (i.e., ~ 1 : 1, see Table IV).

2. In the CO/O_2 and CO/air flames, [OH] was first estimated from the observed initial decay rates of CO on the basis[22] that

$$\frac{-d[CO]}{dt} = k_{CO}\,[CO]\,[OH] \qquad (19)$$

where[42] $$k_{CO} = 5 \times 10^{-13} \exp(-600/RT) \text{ cc sec}^{-1} \qquad (20)$$

Next, since CO and CO_2 were observed (see Fig. 11) to reach steady-state values at about their equilibrium ratio, we reasoned that the reaction

$$OH + CO \rightleftarrows CO_2 + H \qquad (21)$$

---

* It is perhaps relevant to note that reactions between O (and presumably H) atoms and unsaturated perfluorocarbons are known to be rapid.[41] It therefore seems highly likely that equivalent reactions with perfluorocarbon free radicals are also rapid, as we infer from the results of the present study.

is essentially equilibrated in the post-flame gases. Thus,

$$[H] = K_{CO/CO_2}\left(\frac{[CO]}{[CO_2]}\right)\ [OH] \qquad (22)$$

where K_{CO/CO_2} is the equilibrium constant for Eq. (21). (Upon further verification, this novel and simple method for estimating mean values of [OH] and [H] should prove most useful in future combustion studies.)

The observed decay rates are best interpreted as corresponding to the reaction

$$H + C_8F_{18} \xrightarrow{k_H} HF + C_8F_{17} \qquad (23)$$

Values of k_H are shown in Table VIII. We note that efforts to explain the observed results in terms of other reaction partners fail to rationalize the data.* Using procedures reviewed by Semenov (Ref. 43, p. 29 ff.), we estimate the activation energy for Eq. (23) to be ~ 4 kcal mole^{-1}. Values of $k_H/\exp(-4000/RT)$ are also shown in Table VIII, from which we conclude that

$$k_H = (4 \pm 1.3) \times 10^{-11} \exp(-4000/RT)\ \text{cc sec}^{-1} \qquad (24)$$

Reasons for not guessing the temperature exponent of the pre-exponential factor in Eq. (24) without more definitive information are suggested elsewhere.[44, 45]

2. Sulfur hexafluoride.- This substance decomposed anomalously slowly in the environments of the present study; representative decay profiles are shown in Figs. 10 and 11. Fenimore and Jones[12] had previously observed that SO_2 is formed in flames at about the same rate at which SF_6 decomposes. Our observations are similar in this regard: the spectrum of SF_x ion fragments remained essentially unchanged as decomposition progressed, indicating that reactions leading to final products are rapid relative to the initial decomposition reaction in the present environments. Fenimore and Jones, however, interpreted their decomposition results in terms

---

* The rapid C_8F_{18} decay rates observed in the H_2-rich regions of the H_2/O_2 flame (Fig. 10) clearly indicate that OH was not the dominant C_8F_{18} reaction partner in these studies, since in H_2-rich H_2/O_2 flames, $[H] \gg [OH]$.[43]

of a relatively rapid reaction between SF_6 and H atoms; this we do not confirm, as evidenced by the very slow rate of SF_6 decay observed in the H_2/O_2 flame (Fig. 10). Indeed, efforts to rationalize the slow SF_6 decomposition rates summarized in Table VIII in terms of a reaction with any single flame species by means of a simple Arrhenius expression all fail. For the reasons discussed below, we have concluded that the dominant (i.e., rate-determining) decomposition reaction in the present environments is

$$M + SF_6 \xrightarrow{k_M} \text{Products} \qquad (25)$$

As discussed below, the rate "constant" k_M in Eq. (25) is apparently strongly enhanced at higher pressures and at lower temperatures by contributions of vibrationally excited states lying near the dissociation continuum. However, at pressures below ~ 40 Torr and temperatures above ~ 2500 K, these states are apparently not populated rapidly enough to materially enhance the basic rate of reaction arising from activation by simple translational energy transfer in encounters between the species M and SF_6 in their ground states. We conclude that at such low pressures and high temperatures,

$$k_M = (3 \pm 1.1) \times 10^{-10} \exp(-70\,000/RT) \text{ cc sec}^{-1} \qquad (26)$$

3. Discussion. - The observed rapid decay rates of C_8F_{18} vapor, when interpreted in terms of reaction with H atoms, are so near to what one would predict a priori that they require little discussion. On the other hand, the anomalously slow observed rates of SF_6 decomposition in the same low-pressure, high-temperature environments as employed in the C_8F_{18} studies come as a surprise in view of the kinetic results reported by Fenimore and Jones,[12] Modica,[13, 49] and Bott, Thompson, and Jacobs[14] at higher pressures and lower temperatures.

Fenimore and Jones measured SF_6 decomposition rates in $H_2/O_2/Ar$, $C_2H_2/O_2/Ar$ and $H_2/N_2O/Ar$ flames at pressures from 80 to 160 Torr and temperatures from 1300 to 1940 K. They concluded that their results were compatible with either a unimolecular decomposition process or a reaction dominated by H atoms. On the basis of their observed apparent activation energy of only 30 kcal mole^{-1} and an estimated bond energy of 65-75 kcal mole^{-1} for SF_6 (i.e., for the reaction $SF_6 \rightarrow SF_5 + F$), Fenimore and Jones rejected unimolecular decomposition as an explanation of their results. They suggest

$$H + SF_6 \xrightarrow{k_H} HF + SF_5 \qquad (27)$$

$$k_H = 3.3 \times 10^{-9} \exp(-30\,000/RT) \text{ cc sec}^{-1} \quad (28)$$

Use of Eq. (28) predicts a value of ~ 6700 sec^{-1} for the product $k_H[H]$ in the H_2/O_2 flame of the present study at 10 Torr, corresponding to the anticipated value of $-d \ln[SF_6]/dt$. From Table VIII and Fig. 10, however, it is evident that the observed value of $-d \ln[SF_6]/dt$ for this flame is only 19 sec^{-1}. Some of the discrepancy could be due to actual flame temperatures in the present study being below adiabatic equilibrium values; however, to totally resolve this discrepancy (and also those indicated below) on this basis alone requires unreasonably low actual flame temperatures. For example, the actual temperature in the H_2/O_2 flame at 10 Torr would have to be ~ 1300 K rather than the adiabatic value of 2486 K. Although this point requires further confirmation, on the basis of both past experience[46,47] and the thermocouple traverses previously mentioned we do not believe that actual flame temperatures in these studies were more than a few hundred K lower than adiabatic equilibrium values. Thus, we are forced to conclude that Fenimore and Jones' reported kinetics are not confirmed by the present observations. Additionally, efforts to rationalize the results shown in Table VIII in terms of H atom-dominated decomposition also fail. When one further considers that Fenimore and Jones' activation energy of 30 kcal $mole^{-1}$ is abnormally high for exothermic H-atom reactions (see, e.g., the compilation of H-atom rate constants given in Ref. 48), one is obliged to conclude that Fenimore and Jones' results probably do correspond, after all, to unimolecular decomposition.* This conclusion is also reinforced by the recent work of Modica[13,49] and of Bott, Thompson, and Jacobs.[14]

Modica has measured SF_6 decomposition kinetics in shock-heated argon at 1060 Torr and at temperatures between 1700 and 2100 K. His results may be written[49] as

$$M + SF_6 \xrightarrow{k_M} SF_5 + F + M \quad (29)$$

$$k_M = 1.5 \times 10^{-11} \exp(-39\,000/RT) \text{ cc sec}^{-1} \quad (30)$$

---

* The possibility that Fenimore and Jones' observations correspond to reactions of H atoms with vibrationally excited (by ~ 30 kcal $mole^{-1}$) states of SF_6--a mechanism not necessarily operative at the low pressures of the present study--cannot be entirely discarded, but seems remote.

Modica[13] recently performed thermodynamic measurements which yielded a value of 65.2 kcal mole^{-1} for the first bond of SF_6; this strongly indicates that the pre-exponential factor of k_M in Eqs. (26) or (30) cannot be written in simple temperature-independent Arrhenius form for the conditions of his experiments. Since, according to all rate theories, E in the expression $k = A(T) \exp(-E/RT)$ must be at least equal to the endothermic heat of reaction, Modica's results indicate an approximately T^{-7} dependence of A(T). Such a strong temperature dependence of A(T) is characteristic of unimolecular decompositions;[50] accordingly, as pressure decreases at constant temperature, k_M in Eqs. (26) or (30) would <u>not</u> be expected to remain constant.

Bott, Thompson, and Jacobs[14] have recently shown that k_M is indeed pressure-dependent. Their studies of SF_6 decomposition kinetics in shock-heated argon were conducted at temperatures in the range 1700-2050 K and at pressures from 100 to 3400 Torr. They interpret their results in terms of unimolecular rate theory and conclude that the energy of the first bond in SF_6 is 75.4 kcal mole^{-1}, which disagrees with the above-cited determination of 65.2 kcal mole^{-1} by Modica. For present purposes, it seems sensible to suggest the use of a mean value for the bond energy of (70 $\pm$ 5) kcal mole^{-1}. At a pressure of 100 Torr (the lowest studied), the experimental results of Bott, Thompson, and Jacobs may be expressed as

$$M + SF_6 \xrightarrow{k_M} SF_5 + F + M \qquad (29)$$

$$k_M = 1.5 \times 10^{-7} \exp(-70\,000/RT) \text{ cc sec}^{-1} \qquad (31)$$

As is evident from Eq. (31), Bott, Thompson, and Jacobs' rate constant (at 100 Torr) has a pre-exponential factor ~ 3 orders of magnitude higher than that for simple collisions (~ 3×10^{-10} cc sec^{-1}), which strongly indicates the participation of vibrationally excited states in their experimental environments. Referring to the values of $k_M/\exp(-70\,000/RT)$ obtained in the present study and summarized in Table VIII, it is evident that the present results are in essential agreement with Eq. (31) <u>only</u> for the CO/air run at 100 Torr and 1666 K. Indeed, at lower pressures and higher temperatures the observed kinetics appear to approach those typical of encounters between species essentially in their ground states, with a "normal" pre-exponential factor of ~ 3×10^{-10} cc sec^{-1}.

A tentative explanation of this otherwise puzzling result is as follows: McCoubrey,[51] in extended studies of vibrational-translational energy transfer, has reported that ~ 1500 collisions are required to transfer one vibrational quantum (presumably from the lowest-lying, triply-degenerate 345 cm^{-1} mode) in SF_6 at 300 K. If we neglect the unknown effects of temperature* and composition excursions,† it is simple to estimate that ~ 1 x 10^5 collisions (i.e., 1500 x 70 000/2.86 x 345) are required to bring SF_6 up to its dissociation continuum by vibrational excitation in the absence of any deactivation whatever. On the basis that excited states near the dissociation continuum are depleted by rapid reaction only, it is then possible to calculate <u>maximum</u> relative contributions to the kinetics by vibrationally excited states as opposed to reactions involving translational activation of species essentially in their ground states. Invoking an operative collision pre-exponential factor of ~ 3 x 10^{-10} cc sec^{-1}, we find that the <u>maximum</u> relative contributions $k_{M,\ vibration}^{max} / k_{M,\ translation} \cong \exp(70\ 000/RT)/10^5$ are of the order of 10 in the highest temperature flames (Table VIII) and of the order of 10^4 in the flame at 1666 K; the ratios of observed values of $k_M/\exp(-70\ 000/RT)$ follow this trend, although absolute k_M values are of course smaller than $k_{M,\ vibration}^{max}$, because non-reactive deactivation of excited states <u>is</u> important.

Thus, we conclude that the results obtained in the present experiments at high temperature (> 2500 K) and low pressure (< 40 Torr) are consistent with relatively slow vibrational excitation in these environments. This unexpected conclusion has significant implications (e.g., slow decomposition kinetics in rarefied environments) and should be exploited in future, more extensive studies.

---

* According to the Landau-Teller theory,[52] the probability of vibrational energy transfer per collision would be proportional to the exponential of a negative term with a reciprocal cube root dependence on T; small temperature exponents would then be anticipated.

† Dilution with Ar would presumably, but not necessarily, increase the required number of collisions. Water apparently[51] has little effect on the number of collisions required.

IV. IMPLICATIONS TO RE-ENTRY

It seems appropriate to note at this point that the present study has pointed to the dominance of translational energy transfer in determining vaporization and vapor decomposition kinetics in low-pressure, high-temperature flames and therefore (presumably) re-entry flow fields. In this section, some applications and extensions of the experimental findings will be discussed briefly.

A. Thermal Accommodation Coefficients of Droplets

Engineering evaluation of droplets as distributed sources of (possibly) electrophilic vapors in re-entry flow fields, as heat sinks, or as heterogeneous recombination sites obviously requires an ability to predict droplet evaporation rates (as well as initial mean droplet sizes; see Ref. 5). As previously discussed (Section I), evaporation rates are directly proportional to values of the prevailing thermal accommodation coefficients in the re-entry flow fields of present concern. We have shown in this study that accommodation coefficients characterizing translational energy exchange between incident high-temperature thermal gas fluxes and liquids can be significantly less than unity, in accord with the theoretical concepts originated by Baule. What, however, would characterize the same process in the free molecular re-entry environment, in which incident fluxes are largely <u>not</u> random, but directed?

We have explored this problem theoretically, using Baule's apparently successful formulation (as modified in Section III.A.5) as an initial basis. A simple extension of Baule's theory leads, after appropriate integration to evaluate the mean value over the entire reflecting surface (using Baule's functions), to the following expression for $\nu_D^{(1)}$, the mean reflection coefficient (for single gas-liquid encounters) for <u>directed</u> gas fluxes incident on spherical surfaces:

$$\nu_D^{(1)} = \frac{\pi \Omega_\mu}{4 b_L^2} \left(1 + \frac{\sigma_m}{\sigma_M}\right)^2 \left[1 - \frac{m}{3M} - \frac{2\left(1 + \frac{\sigma_m}{\sigma_M}\right)\sqrt{\Omega_\mu}}{3\pi b_L}\right] \qquad (32)$$

Combination of Eq. (32) with

$$\alpha_{T,D} = \alpha_T^{(1)} + \left(1 - \alpha_T^{(1)}\right)\left(1 - \nu_D^{(1)}\right) \tag{14a}$$

and

$$\overline{\alpha}_{T,D} = \sum_i x_i \, \alpha_{T,D,i} \tag{33}$$

leads to the predicted values of $\overline{\alpha}_{T,D}$ shown in Table IX for the liquids employed in the present study. The calculations shown are for a dissociated air (i.e., N_2/O) plasma at 5000 K. Other predicted properties, such as relative atomized mean droplet size (based on the correlation discussed in Ref. 5), relative jet Weber number, and relative free molecule flow mean droplet evaporative lifetime, are also shown in Table IX. It is evident that both perfluoro-octane and Freon E-8 jets are predicted to have better break-up characteristics than water, as well as significantly shorter droplet evaporative lifetimes.

B. Low-Pressure, High-Temperature Decomposition Kinetics of Electrophilic Vapors

Evaluation of flight applications in which the decomposition kinetics of electrophilic vapors are crucial parameters is currently needed. To assist such evaluation, we have compiled the interim decomposition mechanisms for SF_6 and C_8F_{18} vapors shown in Table X. However, we stress that:

1. Table X is an <u>interim</u> compilation reflecting our current assessment of what are clearly as yet incompletely understood complex kinetic mechanisms.

2. Table X is specifically restricted to the low-pressure (< 40 Torr), high-temperature (> 2500 K), <u>uncontaminated</u>, dissociated ($[O] > [O_2]$) air re-entry environments of present interest (see Section I). Extrapolation to other regimes is very likely to lead to serious error because of (1) vibrational excitation enhancement of decomposition rates (assumed negligible in Table X on the basis of the results of the present study) and (2) profound kinetic effects of such contaminants as H atoms.

3. Although they are entirely consistent with the results obtained in the present study, the mechanisms shown in Table X are in large part speculative.

As is evident from Table X, much of the requisite thermochemical data is unavailable or in doubt. Where available, we have used JANAF data;[26] when necessary, we have read between the lines in Heicklen's comprehensive halocarbon kinetics and thermochemistry review.[41] Activation energies in Table X have been approximated from the estimated heats of reaction, following the simple techniques of Semenov.[43] In the Arrhenius expression $k = A \exp(-E/RT)$, A has been estimated as follows: (1) for reactions with appreciable activation energy, A has arbitrarily been estimated as half the hard-sphere collision factor at 2500 K (largely on the basis of the SF_6 decomposition results obtained in this study) and (2) for O atom reactions with low activation energy, A has been estimated from the theory of Kurzius and Boudart,[45] using structural and spectroscopic parameters obtained (or estimated) largely from compilations by Svehla[27] and JANAF.[26]

Restraint has been exercised in selecting what we believe to be the kinetically most significant reactions, since decomposition kinetics must be incorporated into already exceedingly complex computational schemes. Finally, although reactions involving charged species are not considered here, they are obviously essential to the full exploitation of the interim decomposition mechanisms shown in Table X.

V. CONCLUSIONS AND RECOMMENDATIONS

In the present study of vaporization and decomposition kinetics in high-temperature (1670 to 2660 K), low-pressure (5 to 100 Torr) $H_2/CO/O_2$/air flames, it has been shown that:

1. Translational energy transfer is apparently the rate-limiting process in the kinetics of both droplet vaporization and molecular decomposition for the liquids and vapors studied. Specifically, measured water, perfluoro-octane, and Freon E-8 free molecule droplet evaporation rates

are consistent with the effective transfer of translational energy only. Measured SF_6 decomposition rates ($T > 2500$ K; $p < 40$ Torr) are consistent only with reactions not involving vibrationally excited states--which is contrary to observations of other workers at lower temperatures and higher pressures.

2. Measured translational thermal accommodation coefficients of water (0.76 ± 0.14), perfluoro-octane (0.17 ± 0.04), and Freon E-8 (0.22 ± 0.10) are in agreement, within the limits of the data, with predictions based on Baule's classical theory (as reinterpreted in this study).

3. Extension of Baule's theory to directed (as opposed to random) incident gas molecular fluxes leads to the following predictions of translational thermal accommodation coefficients for spherical droplets in dissociated air at 5000 K: water, 0.79; perfluoro-octane, 0.30; Freon E-8, 0.47.

4. Sulfur hexafluoride decayed slowly in the environments of the present study, whereas perfluoro-octane decayed relatively rapidly. Under these conditions, SF_6 is apparently inert to free radical (i.e., H, O, OH) attack; C_8F_{18}, however, reacts rapidly with H atoms. The observed decomposition kinetics are expressed by the following rate-determining reactions and rate constants:

$$M + SF_6 \rightarrow \text{Products};$$

$$k = 3 \times 10^{-10} \exp(-70\,000/RT) \text{ cc sec}^{-1} (T > 2500 \text{ K}; p < 40 \text{ Torr})$$

$$H + C_8F_{18} \rightarrow \text{Products};$$

$$k = 4 \times 10^{-11} \exp(-4000/RT) \text{ cc sec}^{-1}$$

We offer the following recommendations:

1. Studies of the effectiveness of non-equilibrium attachment of free electrons to electrophilic vapors (such as SF_6 and C_8F_{18}) in high-temperature ($T > 3000$ K), low-pressure ($p < 40$ Torr), oxidizing environments are urgently required to assess the degree to which such vapors can enhance homogeneous de-ionization rates in re-entry. Interpretation of the results of such studies in terms of kinetic mechanisms and rate constants is essential for their rational extrapolation to re-entry plasma sheaths, especially since the latter cannot be duplicated in ground test facilities.

2. As the necessary inputs become available, optimizing flow-field flight support calculations of externally injected liquid jet effects on re-entry blackout suppression obviously must eventually incorporate: (1) jet penetration, breakup, and distribution, (2) droplet vaporization and heterogeneous de-ionization kinetics, and (3) vapor decomposition and homogeneous de-ionization kinetics. We recommend that the results of this study be incorporated in such calculations and for this purpose we include suggested interim SF_6 and C_8F_{18} vapor decomposition mechanisms and rate constants for use in low-pressure, high-temperature, uncontaminated Earth re-entry flow field calculations, as well as predicted thermal accommodation coefficients of candidate liquids in the environment of interest.

3. Baule's apparently successful theory, as extended herein, permits a priori prediction of thermal accommodation coefficients in high-temperature gas-liquid encounters. Extension and exploitation of the experimental techniques developed in this work is urged in order to better assess the limitations of (and thus to refine) the theory. Improving the quality of the measurements (e.g., by using holography) would be most desirable.

4. On the basis of our finding that participation of vibrationally excited states is much less likely in reactions at low pressures and high temperatures than in more usually accessible experimental regimes, it is suggested that kinetic mechanisms intended for use in such environments be re-examined in terms of the degree to which incorporated rate constants implicitly, and perhaps erroneously, include large contributions due to excited states.

5. After identification of successful candidate re-entry blackout suppressants (other than water), the kinetics of their decomposition and de-ionization mechanisms should be studied in depth in order to optimize performance. Pressure, composition, and temperature regimes employed in such studies must, however, overlap the regimes of practical interest for the results to be of use.

AeroChem Research Laboratories, Inc.
a subsidiary of Ritter Pfaudler Corporation
Princeton, N.J., 15 August 1968.

REFERENCES

1. Huber, P.W. and Sims, T.E., "The Entry-Communications Problem," Astronaut. Aeron., October 1964, pp. 30-40.

2. Huber, P.W. and Sims, T.E., "Research Approaches to the Problem of Re-Entry Communications Blackout," Proceedings of the Third Symposium on the Plasma Sheath - Plasma Electromagnetics of Hypersonic Flight, Vol. II, eds. W. Rotman et al. (AFCRL-67-0280, SR 64; Air Force Cambridge Research Laboratories, L.G. Hanscom Field, Bedford, Mass., May 1967), pp. 1-33.

3. Cuddihy, W.F., Beckwith, I.E. and Schroeder, L.C., "Flight Test and Analysis of a Method for Reducing Radio Attenuation During Hypersonic Flight," NASA TM X-1331, March 1967.

4. Huber, P.W., "Relation Between Re-Entry Plasma Knowledge and Flight Data," Proceedings of the Conference on the Applications of Plasma Studies to Re-Entry Vehicle Communications, Vol. I (Ohio State University ElectroScience Laboratory, Wright-Patterson Air Force Base, Dayton, Ohio, October 1967), Session II.

5. Kurzius, S.C. and Raab, F.H., "Measurement of Droplet Sizes in Liquid Jets Atomized in Low-Density Supersonic Streams," AeroChem TP-152, Final Report, March 1967.

6. Oppenheim, A.K., "Generalized Theory of Convective Heat Transfer in a Free Molecule Flow," J. Aeron. Sci. 20, 49-58 (1953).

7. Wright, P.G., "The Effects of the Transport of Heat on the Rate of Evaporation of Small Droplets. I. Evaporation into a Large Excess of a Gas," Proc. Roy. Soc. (Edinburgh) 66, 65-80 (1962).

8. Knudsen, M., " Die molekulare Wärmeleitung der Gase und der Akkommodationskoeffizient," Ann. Physik 34, 593-656 (1911).

9. Alty, T. and Mackay, C.A., "The Accommodation Coefficient and the Evaporation Coefficient of Water," Proc. Roy. Soc. (London) A149, 104-116 (1935).

10. Wachman, H.Y., "The Thermal Accommodation Coefficient: A Critical Survey," ARS J. 32, 2-12 (1962).

11. Trilling, L., Wachman, H.Y. and Scott, P.B., "On Accommodation Coefficients," Arch. Mech. Stosowanej 3, 16, 745-760 (1964).

12. Fenimore, C.P. and Jones, G.W., "Decomposition of Sulphur Hexafluoride in Flames by Reaction with Hydrogen Atoms," Combustion and Flame 8, 231-234 (1964).

13. Modica, A.P., "Chemical Kinetics for Air-Teflon and Sulfur Hexafluoride Re-Entry," AMRAC Proceedings, Vol. XVIII, Part I, April 1968, AD390 700, pp. 503-524.

14. Bott, J.F., Thompson, W.P. and Jacobs, T.A., "Chemical Kinetics of Wake Quenchants," ibid., pp. 525-529.

15. Dimmock, N.A., "Production of Uniform Droplets," Nature 166, 686-687 (1950).

16. Schotland, R.M., "Experimental Results Relating to the Coalescence of Water Drops with Water Surfaces," Disc. Faraday Soc. 30, 72-77 (1960).

17. Mason, B.J., Jayaratne, O.W. and Woods, J.D., "An Improved Vibrating Capillary Device for Producing Uniform Water Droplets of 15 to 500 μm Radius," J. Sci. Instr. 40, 247-249 (1963).

18. Lindblad, N.R. and Schneider, J.M., "Production of Uniform-Sized Liquid Droplets," J. Sci. Instr. 42, 635-638 (1965).

19. Schneider, J.M., Lindblad, N.R., Hendricks, C.D., Jr. and Crowley, J.M., "Stability of an Electrified Liquid Jet," J. Appl. Phys. 38, 2599-2605 (1967).

20. Rayleigh, Lord, "On the Instability of Jets," Proc. London Math. Soc. 10, 4-13 (1878).

21. Kurzius, S.C. and Raab, F.H., "Measurement of Gaseous and Heterogeneous Ionization Decay Rates in Nitric Oxide-Seeded Low-Pressure Flames," AeroChem TP-155, Final Report, May 1967.

22. Fristrom, R.M. and Westenberg, A.A., Flame Structure (McGraw-Hill, New York, 1965).

23. Thompson, B.J., Ward, J.H. and Silverman, B.A., "A Laser Fog Disdrometer," J. Appl. Meterorology 3, 792-801 (1964).

24. Gaydon, A.G., The Spectroscopy of Flames (Chapman and Hall, London, 1957).

25. Kaskan, W.E., "The Dependence of Flame Temperature on Mass Burning Velocity," Sixth Symposium (International) on Combustion (Reinhold Press, New York, 1957), pp. 134-143.

26. JANAF Thermochemical Tables (Dow Chemical Corporation, Midland, Mich.), December 1967.

27. Svehla, R.A., "Estimated Viscosities and Thermal Conductivities of Gases at High Temperatures," NASA TR R-132, 1962.

28. Moelwyn-Hughes, E.A., Physical Chemistry, 2nd ed. (Pergamon Press, New York, 1961).

29. Hirschfelder, J.O., Curtiss, C.F. and Bird, R.B., Molecular Theory of Gases and Liquids (Wiley, New York, 1954).

30. Reid, R.C. and Sherwood, T.K., The Properties of Gases and Liquids (McGraw-Hill, New York, 1958).

31. 3M Brand Inert Fluorochemical Liquids (3M Company, St. Paul, Minn., 1965).

32. "Freon" E Series Fluorocarbons (Technical Bulletin No. EL-8A: E.I. du Pont de Nemours, Wilmington, Del., 1966).

33. Clusius, K. and Weigand, K.," Die Schmelzkurven der Gase Ar, Kr, Xe, CH_4, CH_3D, CD_4, C_2H_4, C_2H_6, COS und PH_3 bis 200 Atm. Druck. Der Volumensprung beim Schmelzen," Z. physik. Chem. B46, 1-37 (1940).

34. Brock, J.R., "Evaporation and Condensation of Spherical Bodies in Noncontinuum Regimes," J. Phys. Chem. 68, 2857-2862 (1964).

35. Smoluchowski de Smolan, M., "On Conduction of Heat by Rarefied Gases," Phil. Mag. and Jour. Sci. 46 (Ser. 5), 192-206 (1898).

36. Spalding, D.B., Convective Mass Transfer (McGraw-Hill, New York, 1963).

37. Eckert, E.R. and Drake, R.M., Heat and Mass Transfer, 2nd ed. (McGraw-Hill, New York, 1959).

38. Mills, A.F., "The Condensation of Steam at Low Pressures," University of California, Berkeley, PB175 703, November 1965.

39. Kuhns, I.E. and Mason, B.J., "The Supercooling and Freezing of Small Water Droplets Falling in Air and Other Gases," Proc. Roy. Soc. A302, 437-452 (1968).

40. Baule, B., "Theoretische Behandlung der Erscheinungen in verdünnten Gasen," Ann. Physik 44, 145-176 (1914).

41. Heicklen, J., "Gas Phase Oxidation of Perhalocarbons," Advances in Photochemistry, Vol. 7 (in press).

42. Dixon-Lewis, G., Wilson, W.E. and Westenberg, A.A., "Studies of Hydroxyl Radical Kinetics by Quantitative ESR," J. Chem. Phys. 44, 2877-2884 (1966).

43. Semenov, N.N., Some Problems in Chemical Kinetics and Reactivity, Vol. I, transl. by M. Boudart (Princeton University Press, 1959).

44. Jensen, D.E. and Kurzius, S.C., "Rate Constants for Calculations on Nozzle and Rocket Exhaust Flow Fields," AeroChem TP-149, March 1967.

45. Kurzius, S.C. and Boudart, M., "Kinetics of the Branching Step in the Hydrogen-Oxygen Reaction," Combustion and Flame 12, 477-491 (1968).

46. Miller, W.J., "Mass Spectrometric Study of Combustion Plasma," AeroChem TL-374, May 1968.

47. Calcote, H.F., Kurzius, S.C. and Miller, W.J., "Negative and Secondary Ion Formation in Low-Pressure Flames," Tenth Symposium (International) on Combustion (The Combustion Institute, Pittsburgh, 1965), pp. 605-619.

48. Trotman-Dickenson, A.F. and Milne, G.E., Tables of Bimolecular Gas Reactions (NSRDS-NBS9, National Bureau of Standards, Washington, 1967).

49. Modica, A.P., "Microwave Measurements of Nonequilibrium Air Plasmas Behind Shock Waves Containing Electrophilic Gases," J. Phys. Chem. 71, 3463-3469 (1967).

50. Johnston, H.S., Gas Phase Reaction Rate Theory (Ronald Press, New York, 1966).

51. Cottrell, T.L. and McCoubrey, J.C., Molecular Energy Transfer in Gases (Butterworths, London, 1961).

52. Landau, L.D. and Teller, E., "Zur Theorie der Schalldispersion," Phys. Zeit. Sowjetunion 10, 34-43 (1936).

TABLE I

INJECTION PARAMETERS

	Water	Perfluoro-octane	Freon E-8
Orifice diameter, μm	70.0	72.0	62.5
Transducer frequency, kHz	10.0	7.5	15.0
Injection pressure, psia	14.7	14.7	14.7
Initial jet velocity, cm sec^{-1}	422	261	316
Initial droplet diameter, μm	147	133	114

TABLE II

FLAME CHARACTERISTICS (EVAPORATION STUDIES)

p_∞ = 10 Torr; ϕ = 7/8

Flame	H_2/O_2	H_2/air	CO/O_2 (a)	CO/air (a)
T, K	2573	2146	2541	2147
Molecular weight, amu	15.3	24.7	34.2	32.3
$\overline{m}N_A$, amu	7.23	22.1	32.4	31.3
c_p, cal g^{-1} K^{-1}	0.679	0.394	0.320	0.315
λ, 10^{-4} cal K^{-1} cm^{-1} sec^{-1}	6.45	3.14	3.45	2.92
ℓ_{H_2O}, μm	43.6	44.6	57.3	47.2
$\ell_{C_8F_{18}}$, μm	3.1	3.9	5.7	4.6
ℓ_{E-8}, μm	0.84	1.1	1.6	1.3
Flame gas velocity, cm sec^{-1}	405	284	285	297
Composition (Mole Fractions)				
H	.1062	.0041	-	-
O	.0537	.0025	.0672	.0033
OH	.1018	.0119	-	-
H_2O	.5204	.2851	-	-
H_2	.1267	.0131	-	-
NO	-	.0035	-	.0046
N_2	-	.6562	-	.6486
O_2	.0912	.0235	.1934	.0405
CO	-	-	.3483	.0457
CO_2	-	-	.3911	.2573

[a] These flames were stabilized by addition of 1.3 vol. % methane, the effects of which were omitted from the calculations.

TABLE III

SELECTED NOMINAL LIQUID PROPERTIES[a]

	Water	Perfluoro-octane	Freon E-8
Formula	H_2O	C_8F_{18}	$F(CFCF_3CF_2O)_8CFHCF_3$
Molecular weight, amu	18	438	1448
Purity, vol. %	100	90	[b]20
Vapor pressure, Torr	23.8	30	[b]0.001
Boiling point, K (Normal/10 Torr)	373/284	375/280	[b]570/[b]430
Heat of vaporization, cal g^{-1} (Normal/10 Torr)	540/590	21.1/[b]24.1	9.0/[b]20.1
Specific heat, cal g^{-1} K^{-1}	0.998	0.246	[b]0.235
Density, g cc^{-1} (Normal/10 Torr boiling point)	0.997/1.000	1.77/1.80	1.83/1.58
Viscosity, cP	0.894	1.45	31
Surface tension, dyn cm^{-1}	72.0	14.8	[b]17
ϵ/k, K	809	[b]360	[b]610
σ_M, Å	2.64	[b]7.4	[b]11
a_L[c], Å	3.34	7.94	13.3
b_L (= a_L/σ_M)	1.26	1.07	1.21

[a]At 25°C unless otherwise indicated; property data shown for fluorocarbon liquids are those furnished by the manufacturers (3M Company or du Pont).

[b]Estimated; Freon E-8 property estimates are based largely on extrapolation from smaller homologues of the Freon E series.

[c]At 10 Torr boiling point.

TABLE IV

FLAME CHARACTERISTICS (SF_6 DECOMPOSITION STUDIES)

Flame	H_2/O_2	CO/O_2	CO/O_2	CO/air	CO/air
T, K	2486	2602	2659	2242	1666
p, Torr	10	20	40	40	100
ϕ	0.50	1.09	1.05	1.13	0.58
Flame gas velocity, cm sec^{-1}	678	325	247	240	123
Input Composition (Mole Fractions)					
H_2	.4902	-	-	-	-
CO	-	.6564	.6587	.2792	.1695
CH_4	-	.0071	.0047	.0068	.0034
O_2	.4902	.3282	.3294	.1468	.1695
N_2	-	-	-	.5511	.6373
Ar	.0098	.0034	.0023	.0135	.0102
SF_6	.0098	.0049	.0049	.0027	.0102
Equilibrium Composition (Mole Fractions)					
H	.0408	.0011	.0002	.0005	-
O	.0597	.0548	.0499	.0022	-
F	.0002	.0045	.0130	-	.0288
OH	.0909	.0017	.0004	.0016	-
H_2O	.4182	.0001	-	.0048	-
H_2	.0397	-	-	.0002	-
HF	.0667	.0291	.0210	.0180	.0144
NO	-	-	-	.0041	.0015
N_2	-	-	-	.6111	.6755
O_2	.2616	.1453	.1456	.0214	.0748
CO	-	.3744	.3637	.0606	.0001
CO_2	-	.3795	.3978	.2575	.1834
SO_2	.0111	.0056	.0056	.0030	-
SO_2F_2	-	-	-	-	.0108
Ar	.0111	.0038	.0026	.0150	.0108

TABLE V

OBSERVED DROPLET EVAPORATION RATES

Flame	p_∞, Torr	$\bar{d}$, μm	$-\overline{\Delta d}$, μm	$\overline{\Delta t}$, msec	$-\overline{\Delta d/\Delta t}$, μm sec^{-1}
	Water ($\bar{v}_L$ = 415 cm sec^{-1})				
CO/O_2	5	145	3.4 ± 1.1	20.3	170
CO/O_2	10	141	10.1 ± 1.0	19.1	530
CO/air	10	140	8.8 ± 1.1	20.2	440
H_2/O_2	5	144	9.7 ± 0.8	20.0	490
	Perfluoro-octane ($\bar{v}_L$ = 251 cm sec^{-1})				
CO/O_2	5	99	23	31.8	720
CO/O_2	10	94	58	33.3	1740
CO/air	10	105	29	31.1	940
H_2/O_2	5	87	38	32.2	1180
H_2/air	10	99	47	30.6	1530
	Freon E-8 ($\bar{v}_L$ = 308 cm sec^{-1})				
CO/O_2	5	79	46	26.4	1740
CO/O_2	10	87	58	27.0	2150
CO/air	10	92	33	27.5	1200
H_2/O_2	5	74	64	27.0	2370
H_2/air	10	95	26	27.2	960

TABLE VI

EVAPORATION KINETICS RESULTS

Flame	p_∞, Torr	p_s, Torr	T_∞, K	T_1, K	T_s, K	$\bar{\alpha}_T$ Experiment	$\bar{\alpha}_T$ Theory
Water							
CO/O_2	5	0.6	2484	2430	250	.57	.766
CO/O_2	10	1.2	2541	2350	256	.90	.766
CO/air	10	1.3	2147	1950	257	.82	.725
H_2/O_2	5	0.7	2507	2420	251	.76	.334
Perfluoro-octane							
CO/O_2	5	0.9	2484	2460	248	.18	.141
CO/O_2	10	1.9	2541	2480	255	.21	.141
CO/air	10	1.7	2147	2100	252	.12	.128
H_2/O_2	5	2.0	2507	2480	257	.14	.128
H_2/air	10	2.1	2146	2070	258	.17	.111
Freon E-8							
CO/O_2	5	1.1	2484	2440	383	.37	.283
CO/O_2	10	2.3	2541	2480	391	.24	.283
CO/air	10	2.1	2147	2110	389	.14	.282
H_2/O_2	5	2.7	2507	2470	394	.23	.312
H_2/air	10	2.5	2146	2120	393	.09	.281

TABLE VII

THEORETICAL PRIMARY REFLECTION AND
THERMAL ACCOMMODATION COEFFICIENTS

T_1 = 2500 K

Gas	Water			Perfluoro-octane			Freon E-8		
	$a_T^{(1)}$	$\nu_T^{(1)}$	a_T	$a_T^{(1)}$	$\nu_T^{(1)}$	a_T	$a_T^{(1)}$	$\nu_T^{(1)}$	a_T
H	.100	1.198≡ 1	.100	.005	.842	.162	.001	.641	.360
O	.498	.959	.518	.068	.929	.134	.022	.698	.317
OH	.499	.937	.531	.072	.927	.140	.023	.697	.319
H_2O	.500	.925	.537	.076	.982	.093	.024	.767	.252
H_2	.181	1.236≡1	.181	.009	.881	.127	.003	.667	.335
N_2	.477	.660	.655	.111	.995	.116	.037	.740	.288
NO	.468	.593	.685	.120	.982	.136	.040	.733	.296
O_2	.461	.531	.714	.127	.972	.152	.042	.727	.303
CO	.477	.614	.679	.111	.995	.115	.037	.739	.288
CO_2	.412	.060	.965	.166	1.048≡1	.166	.057	.788	.257

TABLE VIII

OBSERVED DECOMPOSITION RATES

A. Perfluoro-octane

Flame	p, Torr	T, K	x_H, 10^{-3}	$-d \ln [C_8F_{18}]/dt$, 10^3 sec^{-1}	k_H, 10^{-11} cc sec^{-1}	$k_H/\exp(-4000/RT)$, 10^{-11} cc sec^{-1}
H_2/O_2	10	2486	23	1.4	1.6	3.6
CO/O_2	20	2602	2.7	4.8	2.4	5.2
CO/O_2	40	2659	0.85	2.0	1.7	3.6
CO/air	40	2242	0.84	1.2	0.8	2.0

B. Sulfur Hexafluoride

Flame	p, Torr	T, K	$-d \ln [SF_6]/dt$, 10^3 sec^{-1}	k_M, 10^{-16} cc sec^{-1}	$k_M/\exp(-70\,000/RT)$, 10^{-10} cc sec^{-1}
H_2/O_2	10	2486	0.019	4.9	4.0
CO/O_2	20	2602	0.064	8.5	3.8
CO/O_2	40	2659	0.080	5.5	2.0
CO/air	40	2242	0.074	4.3	16
CO/air	100	1666	0.079	1.4	960

TABLE IX

PREDICTED LIQUID PROPERTIES IN FREE MOLECULE RE-ENTRY FLOWS

T_∞ = 5000 K; $T_s \approx$ 10 Torr boiling point

		Water	Perfluoro-octane	Freon E-8
$\nu_D^{(1)}$	O	0.679	0.735	0.527
	O_2	0.136	0.772	0.552
	N_2	0.280	0.794	0.562
$\alpha_{T,D}$	O	0.659	0.315	0.484
	O_2	0.926	0.326	0.471
	N_2	0.854	0.295	0.459
$\overline{\alpha}_{T,D}$ (N_2 + O plasma)		0.786	0.302	0.468
Relative jet Weber number		1	4.9	4.2
Relative atomized mean droplet size[a]		1	0.45	0.47
Relative mean evaporative lifetime[b]		1	0.086	0.041

[a] Based on the correlation discussed in Ref. 5 and properties shown in Table III.

[b] Based on atomized mean droplet size, free molecule evaporation, $\overline{\alpha}_{T,D}$, and properties shown in Table III.

TABLE X

INTERIM DECOMPOSITION MECHANISMS FOR SF_6 AND C_8F_{18} VAPORS IN HIGH-TEMPERATURE UNCONTAMINATED AIR AT LOW PRESSURE

$T > 2500$ K; $p < 40$ Torr
(Vibrational excitation of reactants assumed negligible)
$[O] > [O_2] > [SF_6]$ or $[C_8F_{18}]$

	$\Delta H^o_{f,0}$, kcal mole^{-1}	Estimated Rate Constant $[k = A \exp(-E/RT)]$	
SF_6		A, cc sec^{-1}	E, kcal mole^{-1}
1. $SF_6 + M \rightarrow SF_5 + F + M$	70	3×10^{-10}	70
2. $SF_5 + O \rightarrow SF_4O + F$	[a] -45	1×10^{-11}	0
3. $SF_4O + O \rightarrow SF_3O + OF$	[a] 25	3×10^{-10}	30
4. $SF_3O + O \rightarrow SO_2F_2 + F$	[a] -50	1×10^{-11}	0
5. $SO_2F_2 + O \rightarrow SO_2F + OF$	[a] 35	3×10^{-10}	40
6. $SO_2F + O \rightarrow SO_2 + OF$	[a] 30	3×10^{-10}	35
7. $OF + O \rightarrow O_2 + F$	-65	5×10^{-12}	0
C_8F_{18}			
1. $C_8F_{18} + M \rightarrow 2C_4F_9 + M$	[a] 75	5×10^{-10}	75
2. $C_8F_{18} + O \rightarrow C_8F_{17} + OF$	[a] 60	6×10^{-10}	60
3. $C_nF_{2n+1} + O \rightarrow C_{n-1}F_{2n-1} + CF_2O$ ($n = 2$ to 8)	[a] -95	$9n^{\frac{1}{2}} \times 10^{-12}$	0
4. $CF_3 + O \rightarrow CF_2O + F$	-75	2×10^{-11}	0
5. $CF_2O + O \rightarrow CFO + OF$	80	3×10^{-10}	80
6. $CFO + O \rightarrow CO + OF$	-20	1×10^{-11}	5
7. $OF + O \rightarrow O_2 + F$	-65	5×10^{-12}	0

[a] Estimated, using JANAF thermochemical data where available.[26]

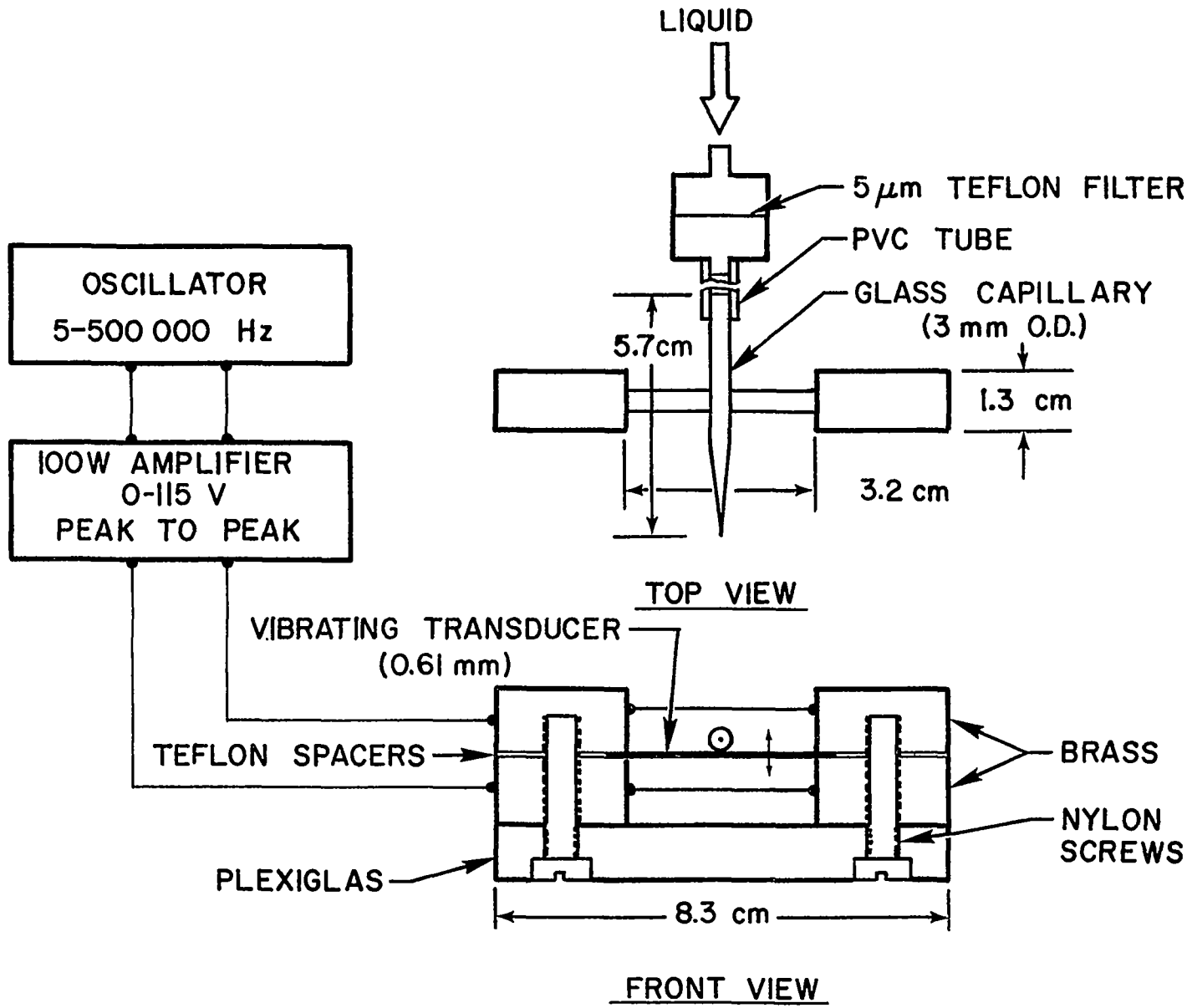

FIG. 1 APPARATUS FOR PRODUCTION OF UNIFORMLY SIZED DROPLETS

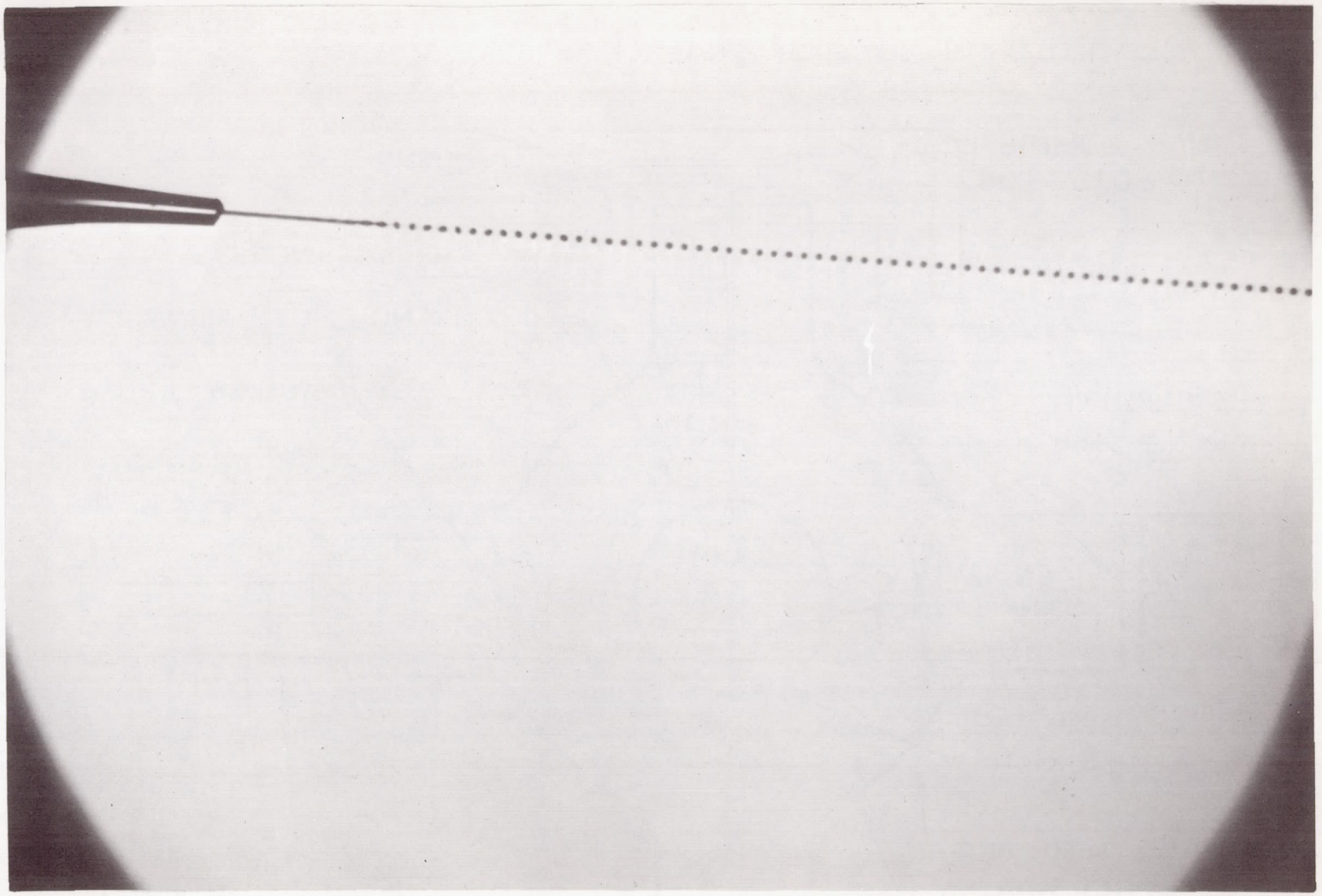

FIG. 2 BREAKUP OF A WATER JET FROM AN ACOUSTICALLY DRIVEN CAPILLARY

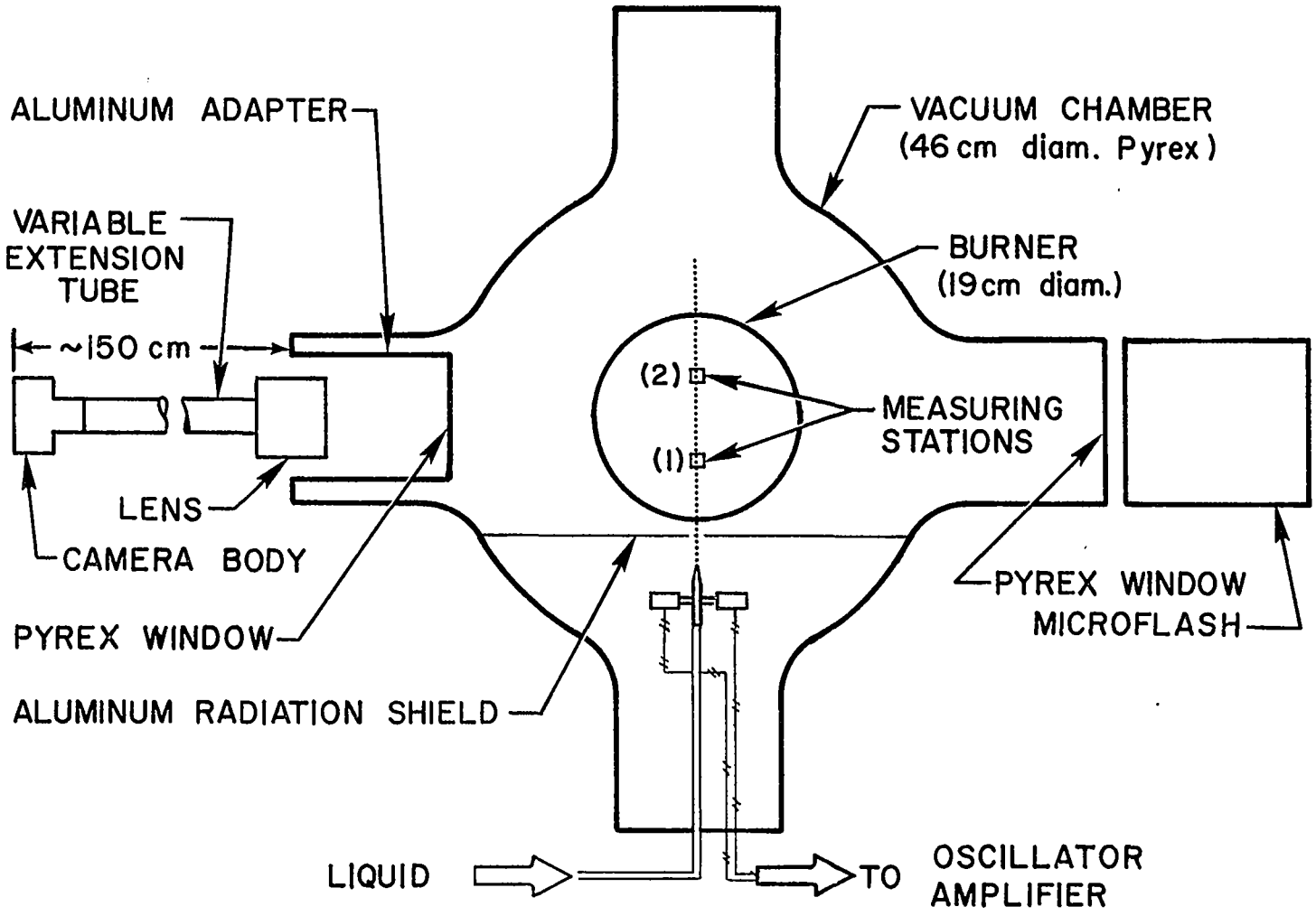

FIG. 3 DROPLET EVAPORATION MEASUREMENT APPARATUS (TOP VIEW)

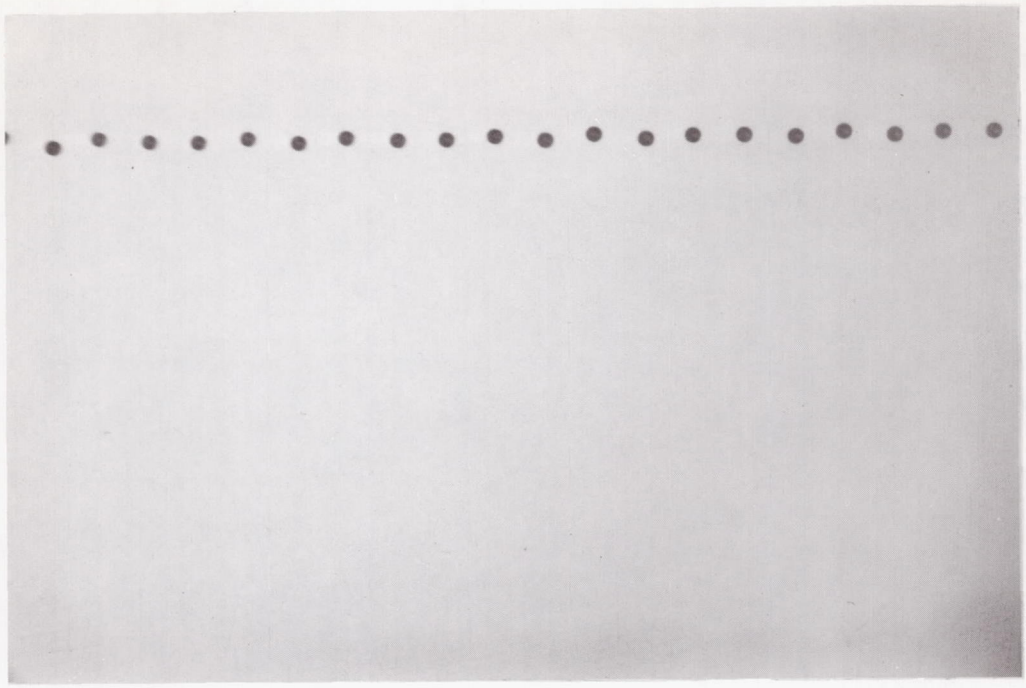

A. STATION 1

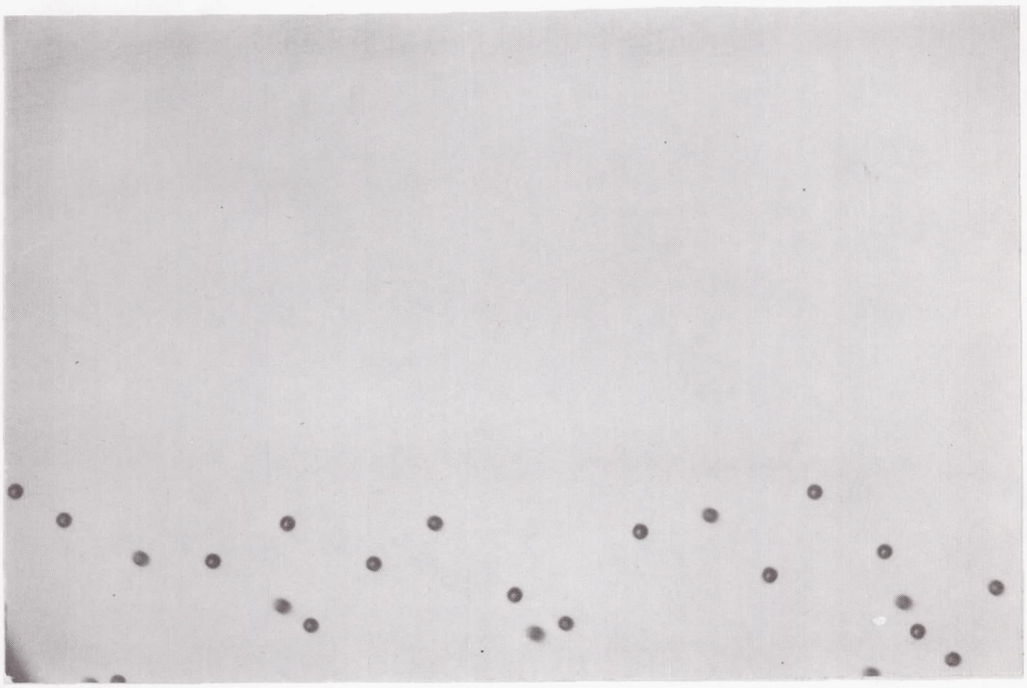

B. STATION 2

FIG. 4 H_2O DROPLETS IN A 10 TORR CO/AIR FLAME

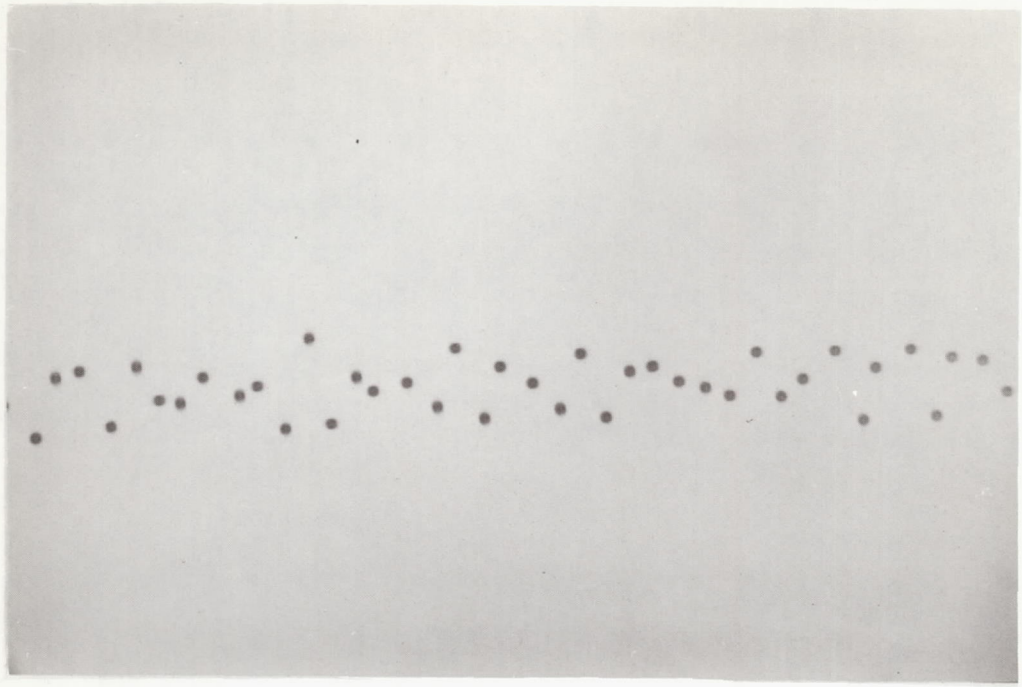

A. STATION 1

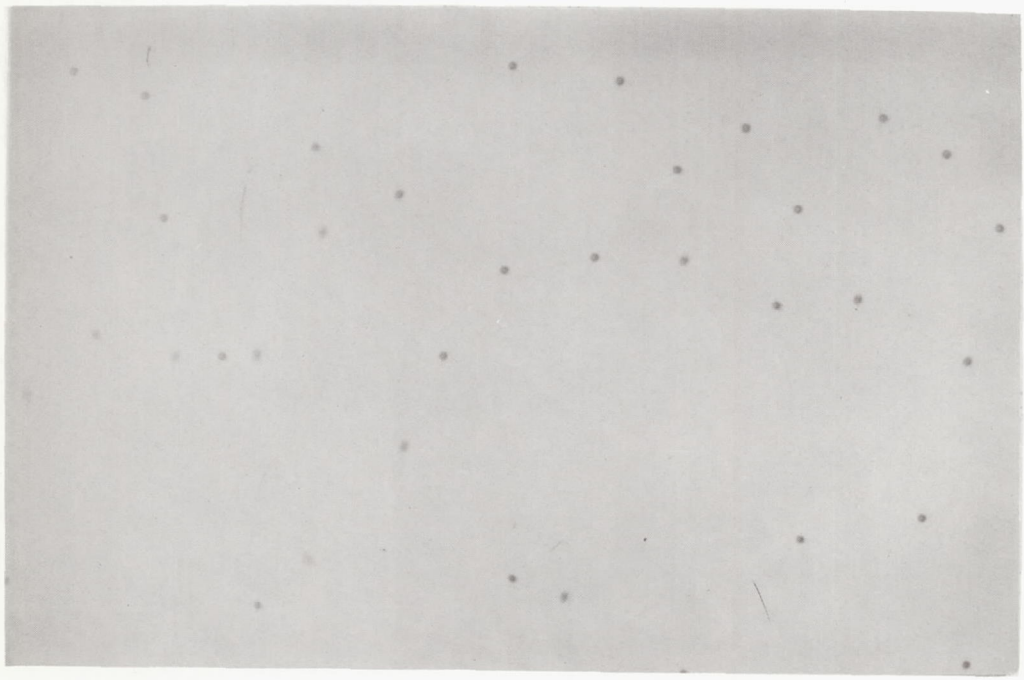

B. STATION 2

FIG. 5 FREON E-8 DROPLETS IN A 10 TORR CO/AIR FLAME

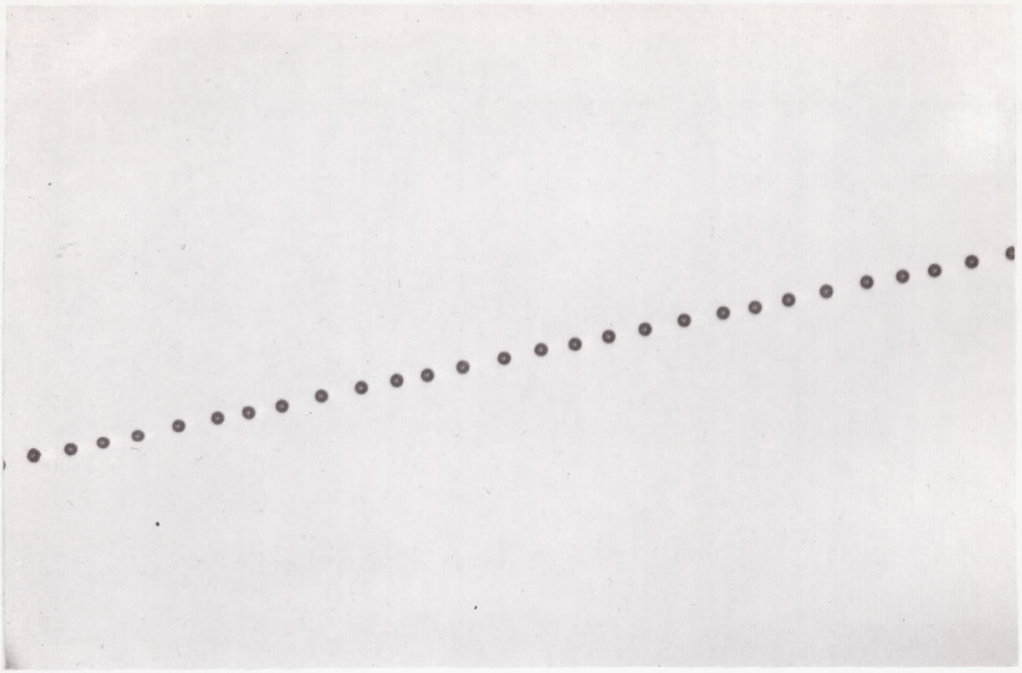

A. STATION 2 (NO FLAME)

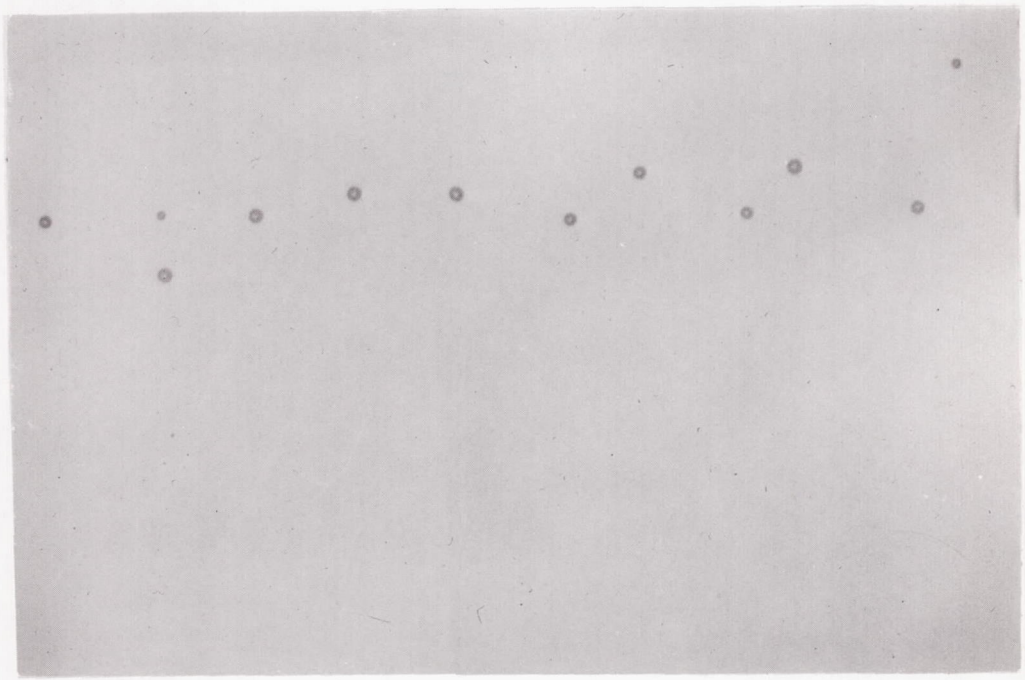

B. STATION 2 (FLAME ON)

FIG. 6 C_8F_{18} DROPLETS IN A 10 TORR CO/AIR FLAME

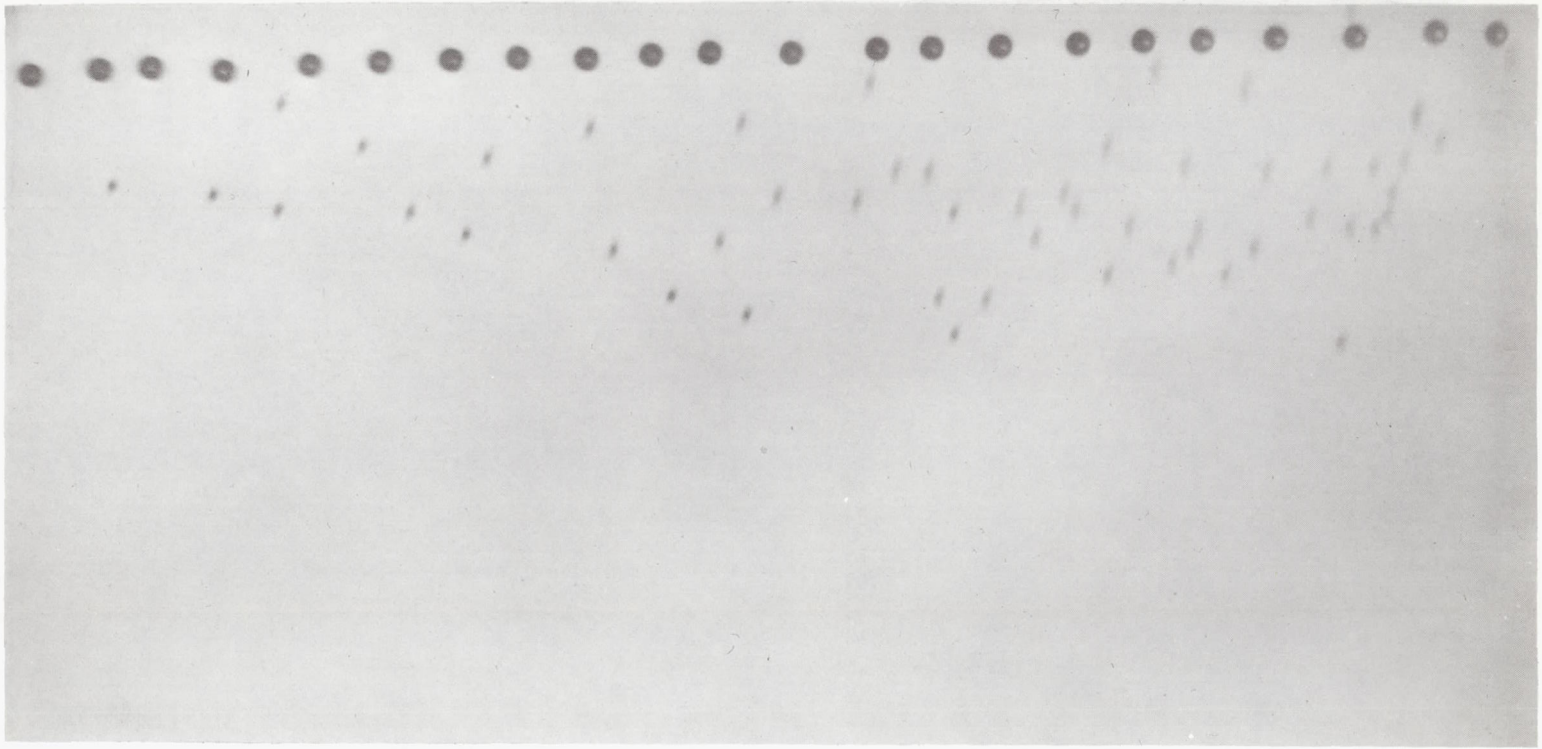

FIG. 7 SATELLITE JET FORMATION IN A JET OF WATER DROPLETS

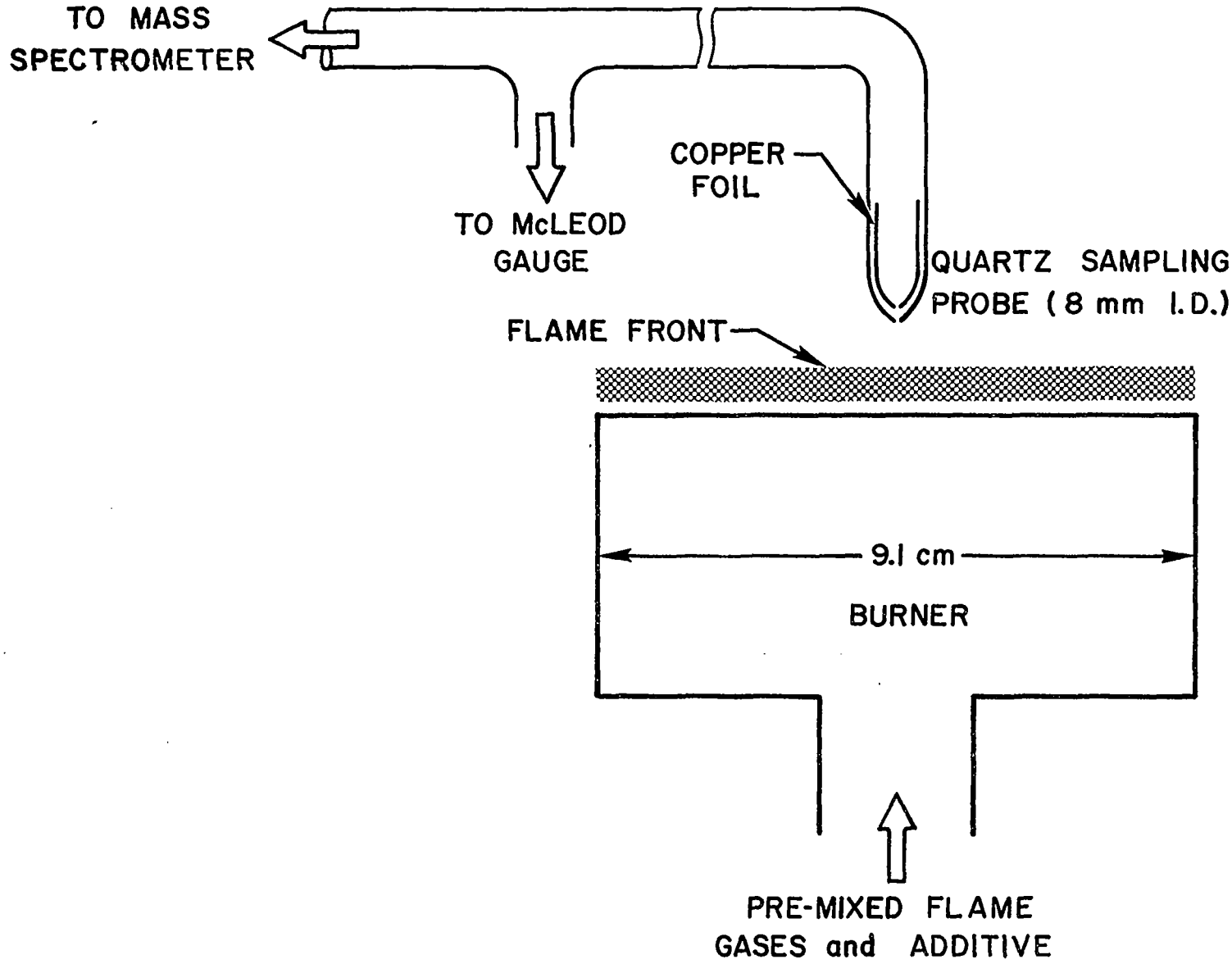

FIG. 8 FLAME GAS ANALYSIS APPARATUS (SIDE VIEW)

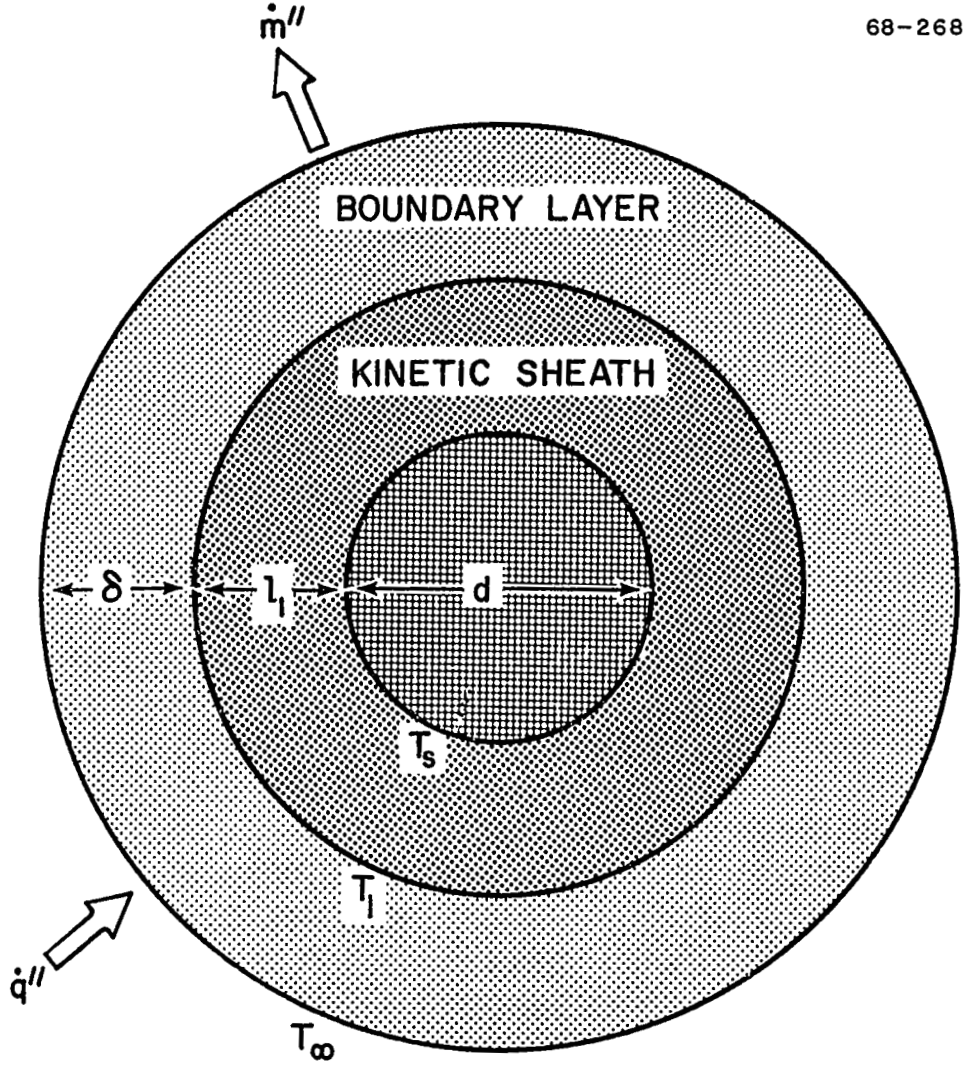

FIG. 9 CONCEPTUAL HEAT TRANSFER MODEL OF AN EVAPORATING DROPLET

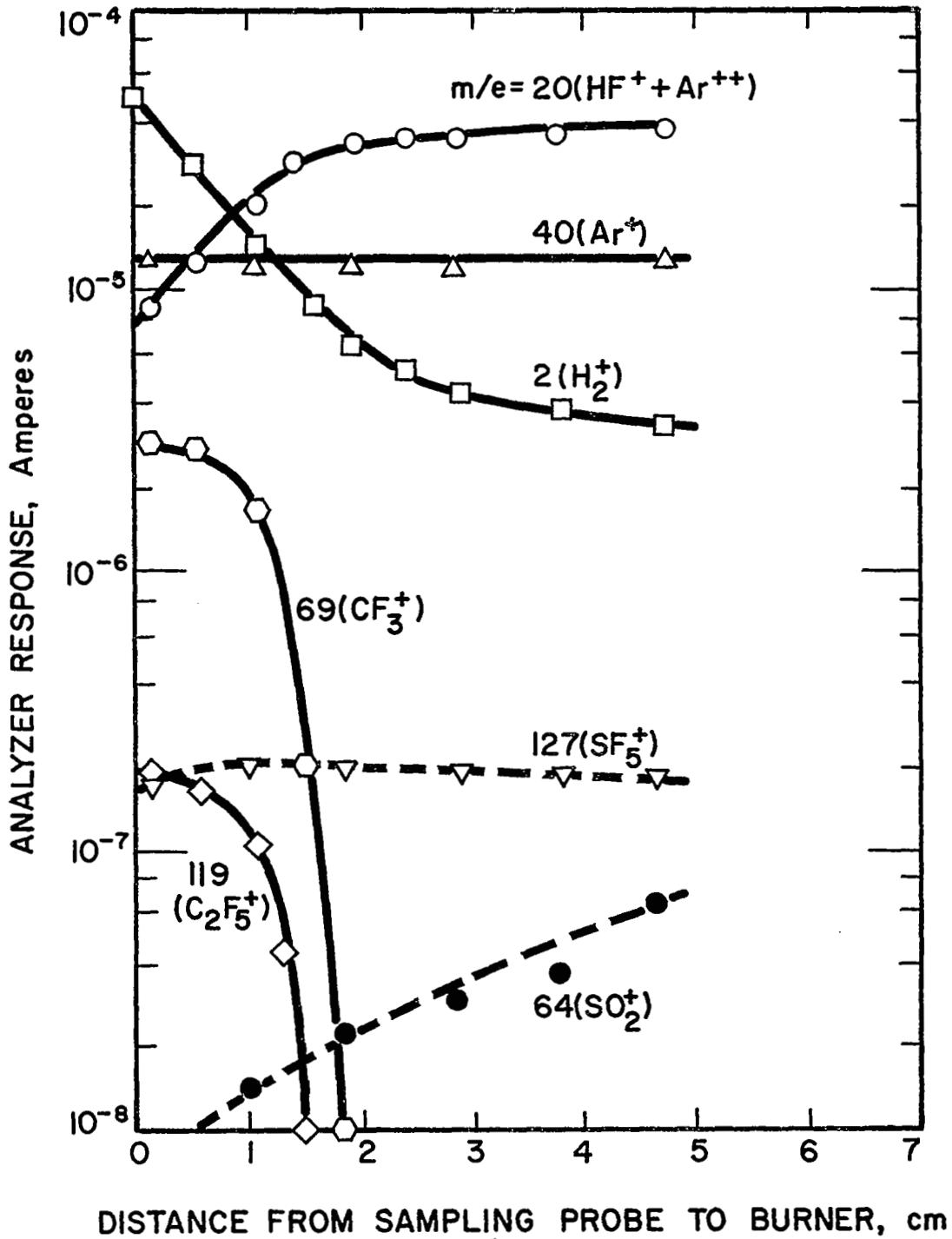

FIG. 10 DECOMPOSITION OF C_8F_{18} AND SF_6 VAPORS IN A 10 TORR H_2/O_2 FLAME

C_8F_{18}: 0.5 vol.% or SF_6: 1.0 vol.% (dashed curves)

(See Table IV for flame characteristics.)

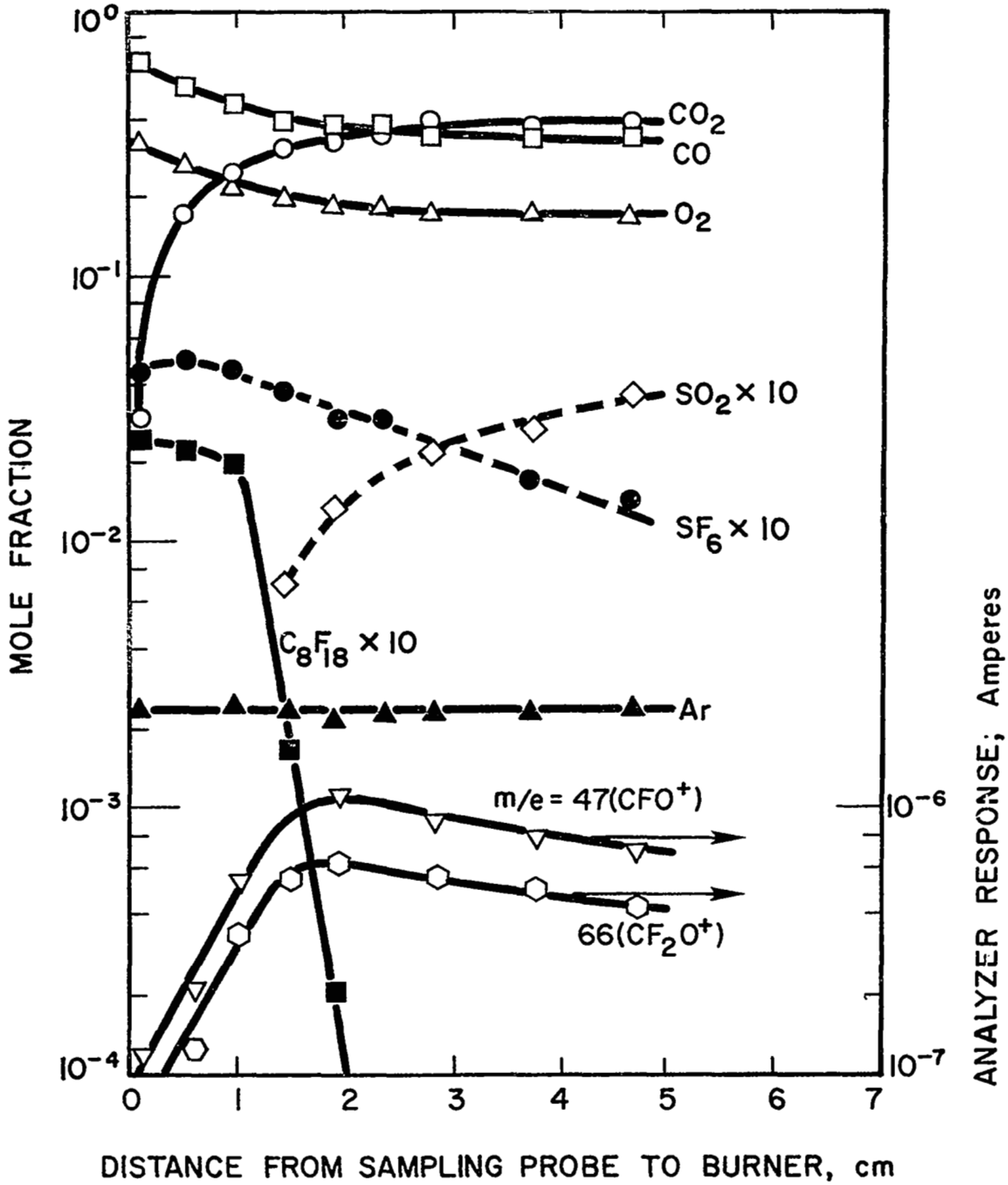

FIG. 11 DECOMPOSITION OF C_8F_{18} AND SF_6 VAPORS IN A 40 TORR CO/O_2 FLAME

C_8F_{18}: 0.25 vol.% or SF_6: 0.5 vol.% (dashed curves)

(See Table IV for flame characteristics.)

NASA-Langley, 1969 — 7 CR-1330